Radar scattering

Computational Light Scattering (PAP315)

Lecture 06

Understanding radar scattering

- Multi-parameter problem: The size, shape, and material of wavelength-scale particles on asteroid surfaces play a role in radar scattering as well as the structure of the sub-surface
- Modeling work is crucial for understanding how to interpret the radar data due to the large parameter space and complex geometric scenarios

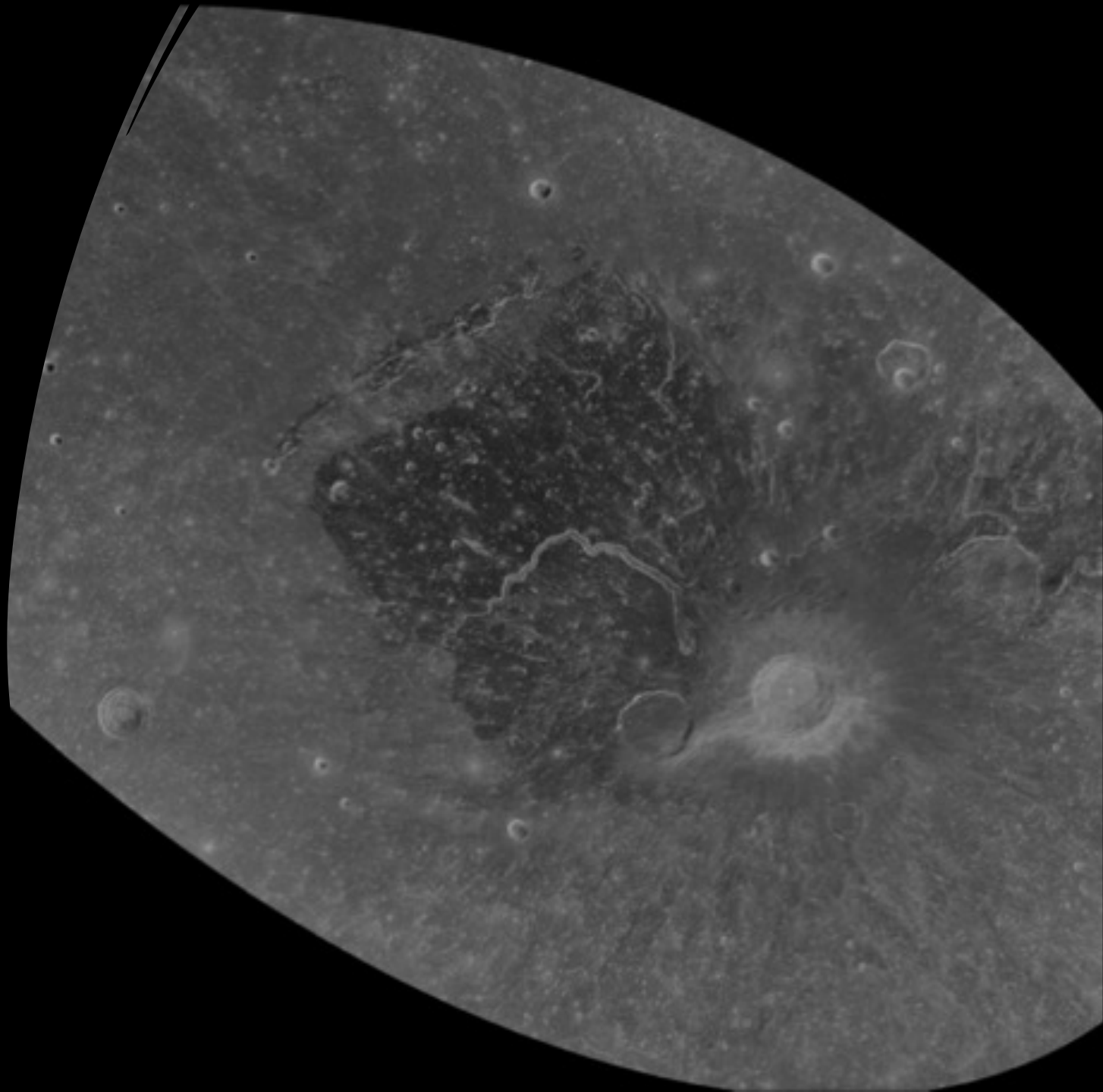

Understanding radar scattering

- The modeling work began in 1960s from analytical solutions for reflectivity of gently undulating surfaces applied empirically to, e.g., the Moon (See Lecture 06 on Scattering by rough surfaces)
- Later more comprehensive analytical models including also elliptical subsurface particles have been developed (e.g., Vector Radiative Transfer (VRT) model introduced by Fa et al. 2011)
- Raney et al. 2012 introduced the **m-chi decomposition**, a new way to illustrate polarization in radar images by RGB colours together with a set of interpretations for each color
- Understanding radar polarimetry fully requires even more complex models, which requires numerical modeling

Basic concepts – Radar cross section

Radar cross section: $\sigma_{pq} = \dfrac{(4\pi)^3 d^4 (P_{rx,pq} - P_{noise})}{P_{tx} G_{tx} G_{tx} \lambda^2}$

- P_{tx}, P_{rx} = Transmitted and received power
- P_{noise} = Noise power (normal distribution)
- G_{tx}, G_{rx} = Antenna gain (transmitted and received): $4\pi\eta A/\lambda^2$ (η is the radiation efficiency)
- λ = wavelength (e.g., S band ≈ 11-14 cm, X band ≈ 2-5 cm)
- σ_{pq} = radar cross section in a specific polarization (the area of an ideal reflector at the same distance that would reflect as much power back)
- d = distance (note the relative impact due to the power of 4)

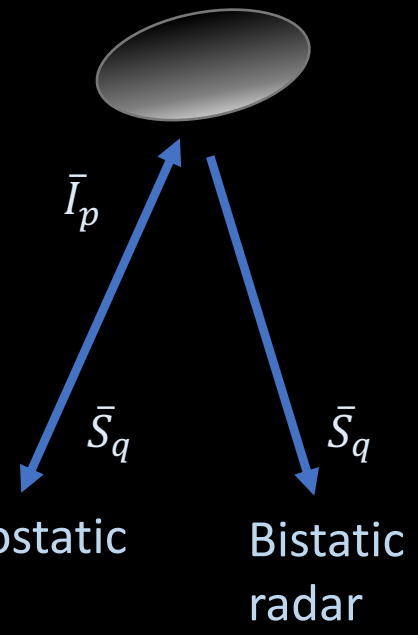

Basic concepts – Backscatter cross section

Backscatter cross section: $\sigma_{pq} = \frac{4\pi \left| A_{pq}(180°) \right|^2}{k^2}$

- A_{pq} = amplitude scattering matrix element pq
- k = wavenumber
- A historical definition that is 4π off from the intuitive definition (the differential energy to the solid angle around the backscatter direction)
  - Thus can be greater than the scattering cross section!

Backscatter efficiency: $Q_{pq} = \frac{\sigma_{pq}}{A_{proj}} = \frac{4\left| A_{pq}(180°) \right|^2}{x^2}$

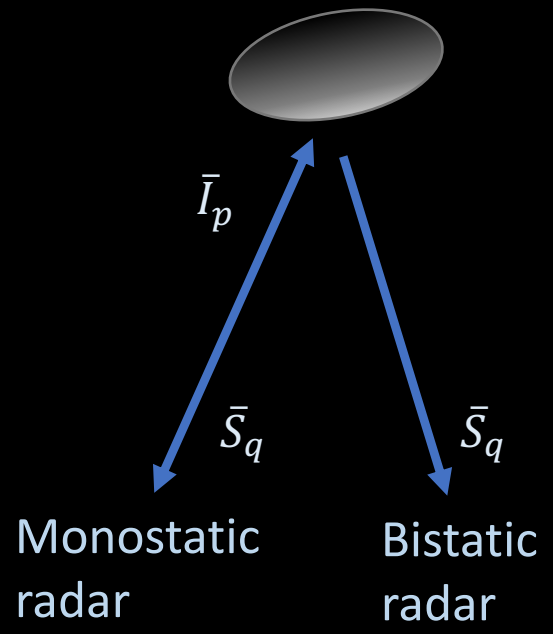

Basic concepts – Backscatter coefficient

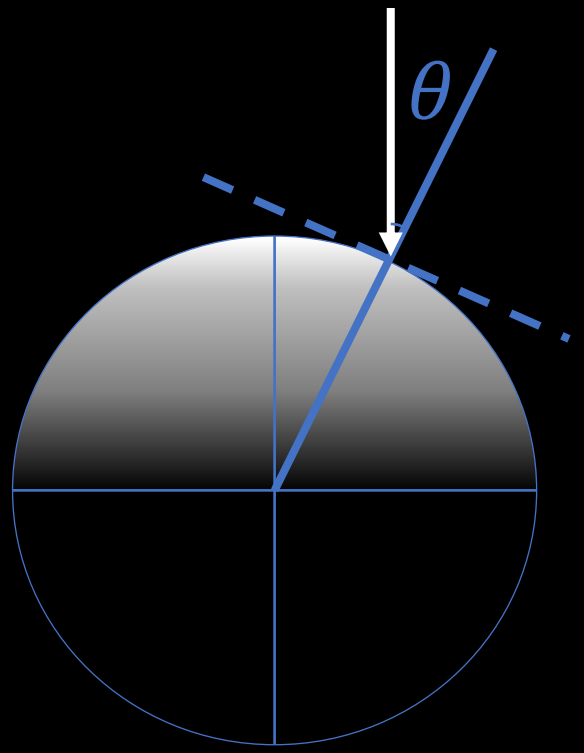

The **backscatter coefficient (BSC)** describes the backscatter cross section of a surface element (of area A).

Incidence angle: The angle between the normal of a surface element and the incident wave (on the left).

The disk function is the BSC as a function of incidence angle (on the right).

Radar albedo: Sphere-integrated BSC divided by the full projected area of a target:

$$\hat{\sigma}_{pq} = \frac{\sigma_{pq}}{A_{proj}}$$

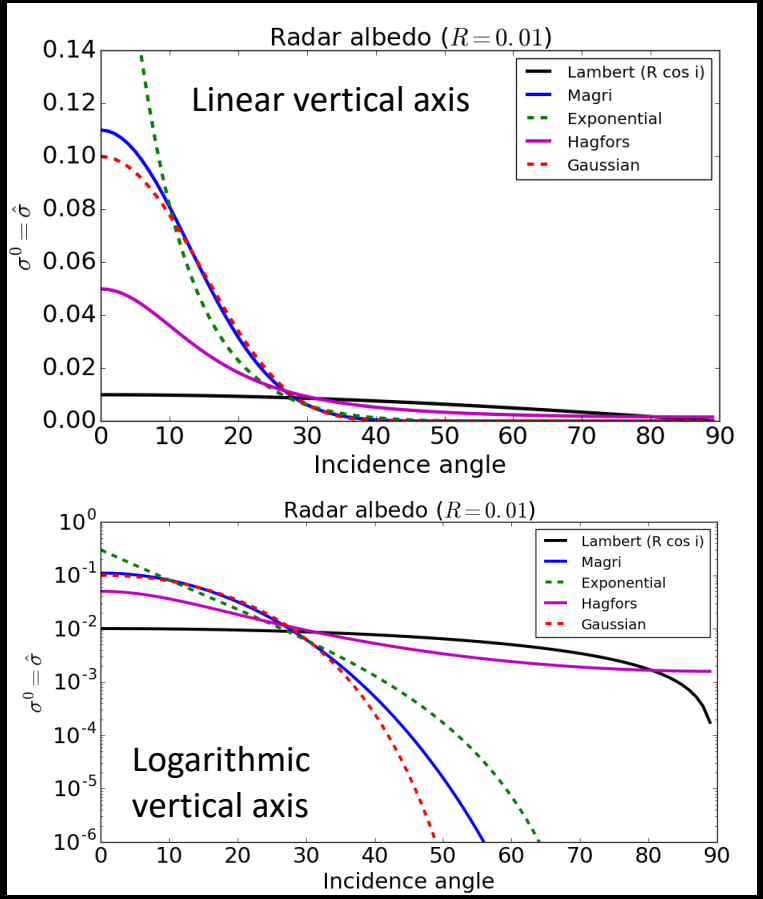

Basic concepts – Backscatter coefficient

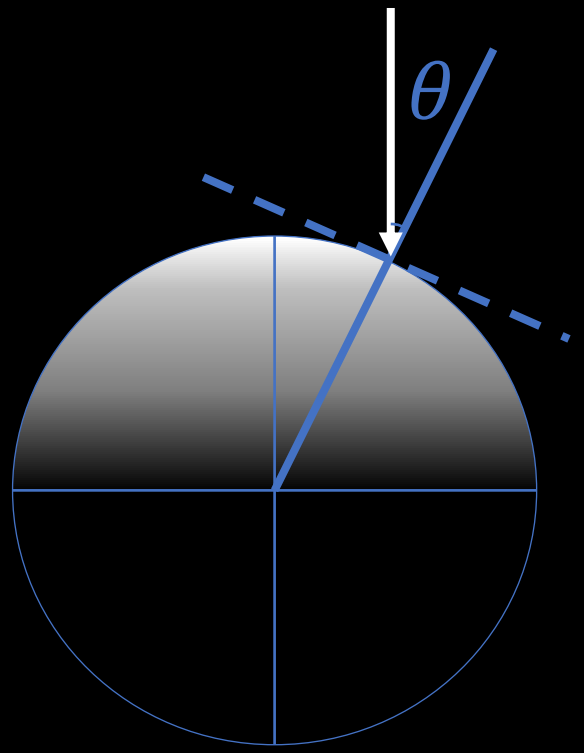

Complications:

- North-South ambiguity
- Asteroids have an unknown shape (incidence angle distribution), whereas planets can be approximated as spheroids
- Differences in scattering between mono- and bistatic systems

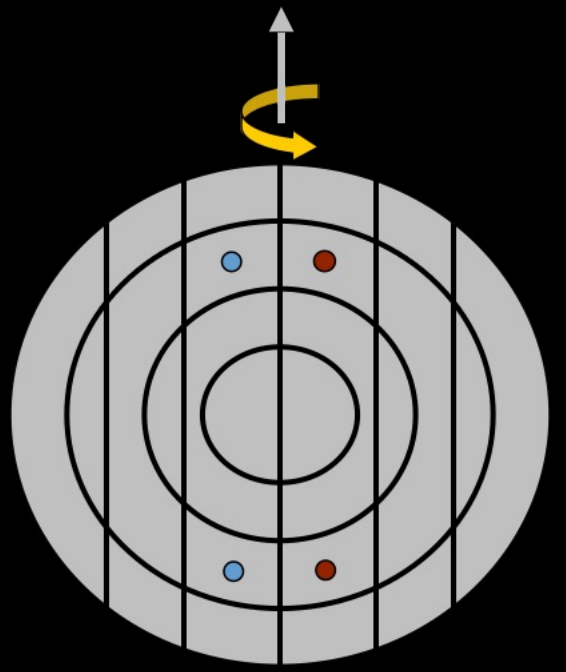

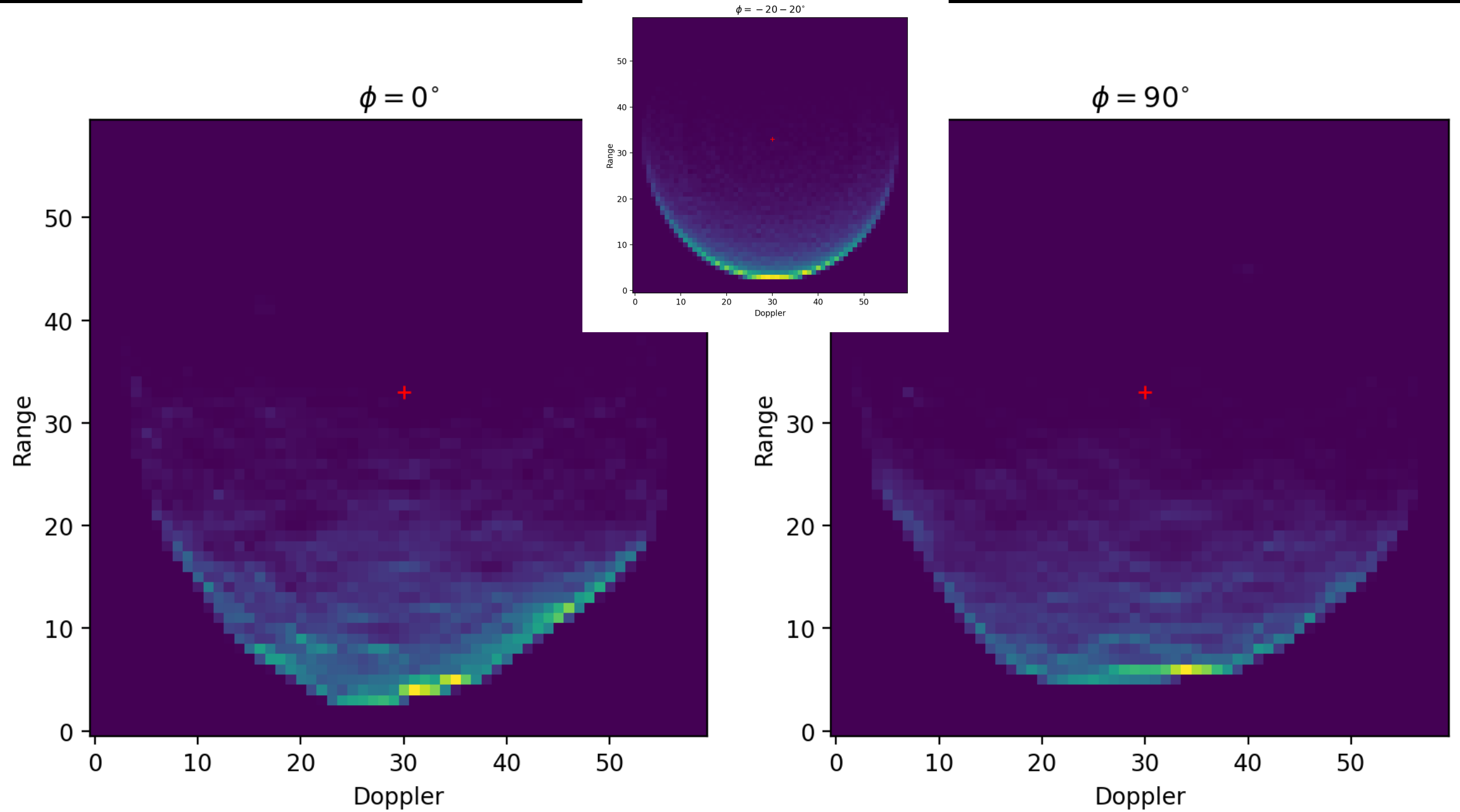
$\phi = -20 - 20^{\circ}$
Range
Doppler
$\phi = 0^{\circ}$
Range
Doppler
$\phi = 90^{\circ}$
Range
Doppler

Basic concepts – polarization

- Radar systems can be set up to use either linear or circular polarization
- Ground-based radar systems use typically circular polarization (the atmosphere rotates the signal a little bit; for circular polarization the amount is not as relevant as for linear polarization)
  - Observations of the electric fields in the **opposite-circular (OC)** and **same-circular (SC)** polarization senses compared to the transmitted signal (a.k.a. **left** and **right** circ. polarization)
- Space-based radar systems use typically linear polarization
  - Observations of the electric fields in the parallel and orthogonal polarizations as the transmitted signal

Basic concepts – polarization

Deriving the Stokes vector elements from the polarization elements:

$$
\begin{aligned}
S_1 &= \langle a_1^2 \rangle + \langle a_2^2 \rangle &&= \langle |E_H|^2 + |E_V|^2 \rangle &&= \langle |E_L|^2 + |E_R|^2 \rangle \\
S_2 &= \langle a_1^2 \rangle - \langle a_2^2 \rangle &&= \langle |E_H|^2 - |E_V|^2 \rangle &&= 2\,Re\,\langle E_L E_R^* \rangle \\
S_3 &= 2\,\langle a_1 a_2 \cos\delta \rangle &&= 2\mathrm{Re}\langle E_H E_V^* \rangle &&= 2\mathrm{Im}\langle E_L E_R^* \rangle \\
S_4 &= -2\,\langle a_1 a_2 \sin\delta \rangle &&= -2\mathrm{Im}\langle E_H E_V^* \rangle &&= -\langle |E_L|^2 - |E_R|^2 \rangle
\end{aligned}
$$

NOTE Here: Backscatter alignment (BSA): typical for observations of macroscale targets or media
Forward scatter alignment (FSA): $-S_4$ (typical for particles and inhomogeneous media)

Basic concepts – polarization

Deriving the polarization components from the scattering matrix elements:

LINEAR

$$\sigma^0_{HH} \propto P_{11} + 2P_{12} + P_{22}$$
$$\sigma^0_{VV} \propto P_{11} - 2P_{12} + P_{22}$$
$$\sigma^0_{HV} \propto P_{11} - P_{22}$$

$$\boxed{\sigma^0_{pq} \propto \bar{S}_q \bar{P} \bar{I}_p}$$

CIRCULAR

$$\sigma^0_{LL} \propto P_{11} + 2P_{14} + P_{44}$$
$$\sigma^0_{LR} \propto P_{11} - P_{44}$$

NOTE:

$$\boxed{\sigma^0 = 4\pi \cos\theta_i \cos\theta_s \, \sigma_{BRDF}}$$

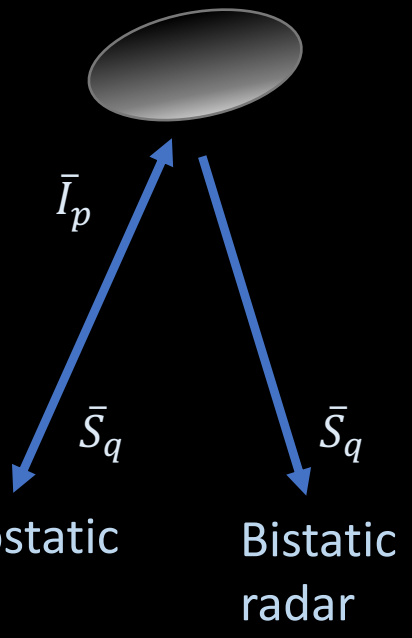

Basic concepts – polarization

Deriving circular polarization from linear polarization:

- Same circular

$$\sigma_{LL}^0 = \frac{1}{4}\left(\sigma_{HH}^0 + \sigma_{VV}^0 - 2\sqrt{\sigma_{HH}^0\sigma_{VV}^0}\langle\cos\delta_{HH-VV}\rangle\right) + \sigma_{HV}^0$$

- Opposite circular

$$\sigma_{LR}^0 = \frac{1}{4}\left(\sigma_{HH}^0 + \sigma_{VV}^0 + 2\sqrt{\sigma_{HH}^0\sigma_{VV}^0}\langle\cos\delta_{HH-VV}\rangle\right)$$

- $\langle\cos\delta_{HH-VV}\rangle$ is the time-averaged phase difference between the HH and VV components

Basic concepts – polarization

- **Smooth surfaces:**
  Specular reflection
  –> All echo in the *opposite-circular* (OC) polarization than the transmitted signal ($p \neq q$)

- **Rough surfaces (wavelength-scale surface roughness or boulders):** Quasi-specular + diffuse scattering
  –> Echo partly in the OC polarization and partly in the *same-circular* (SC) polarization ($p = q$)

$$\mu_C = \frac{\sigma_{SC}}{\sigma_{OC}}$$

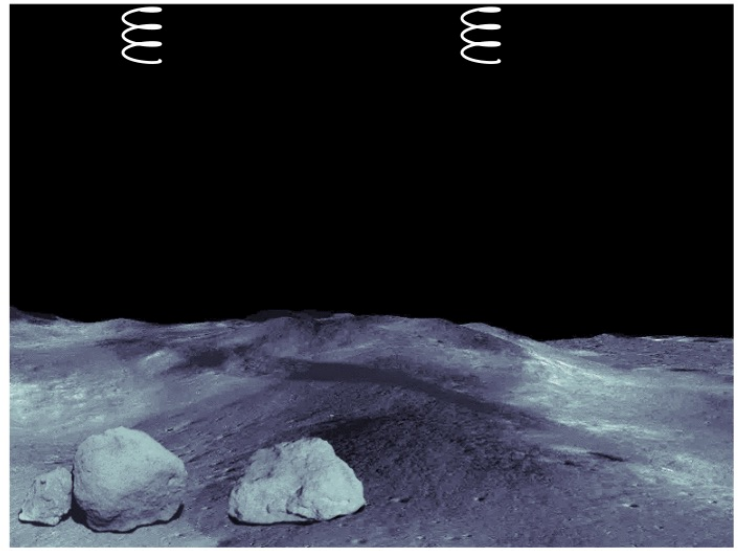

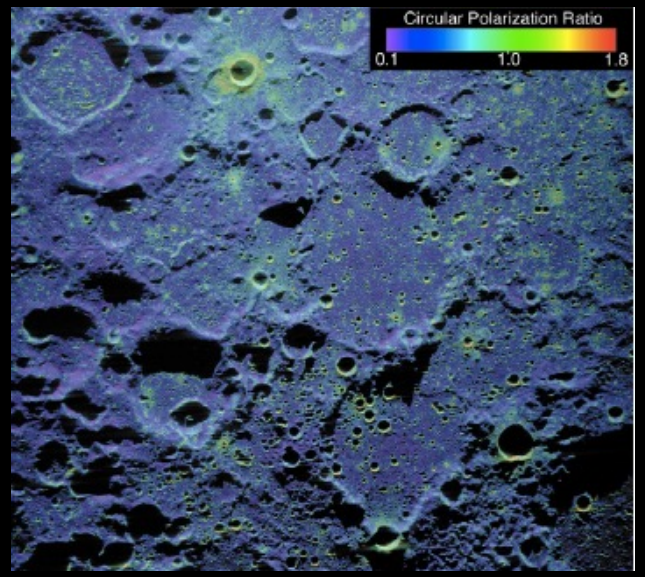
Circular Polarization Ratio
0.1
1.0
1.8

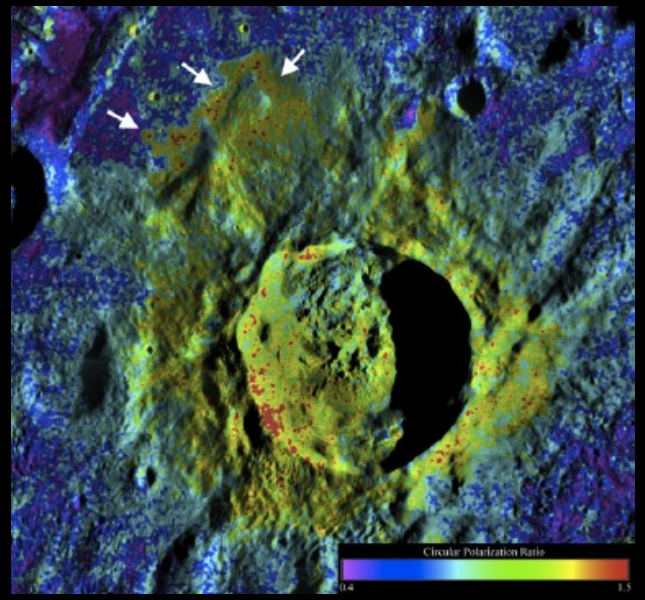
Circular Polarization Ratio

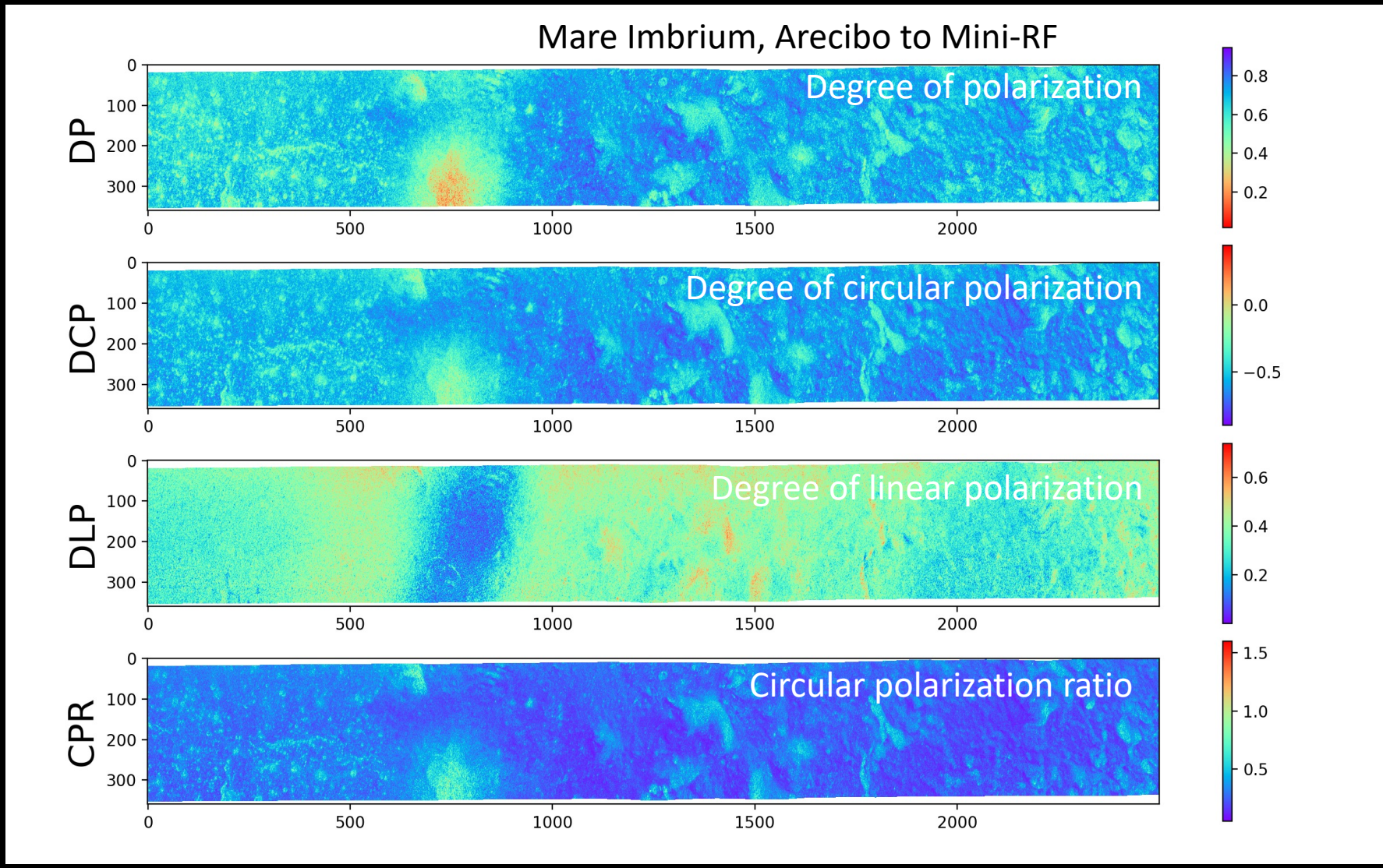
Mare Imbrium, Arecibo to Mini-RF
DP
Degree of polarization
DCP
Degree of circular polarization
DLP
Degree of linear polarization
CPR
Circular polarization ratio
0
100
200
300
500
1000
1500
2000
0.8
0.6
0.4
0.2
0.0
−0.5
1.5
1.0
0.5

m-chi (χ) decomposition

$$\begin{aligned}\text{Red} &= [mS_1(1+\sin 2\chi)/2]^{1/2}\\ \text{Green} &= [S_1(1-m)]^{1/2}\\ \text{Blue} &= [mS_1(1-\sin 2\chi)/2]^{1/2}\end{aligned}$$

Degree of polarization

$$m = \frac{\sqrt{S_2^2 + S_3^2 + S_4^2}}{S_1}$$

$$\chi = \frac{1}{2}\arcsin\left(\frac{S_4}{mS_1}\right)$$

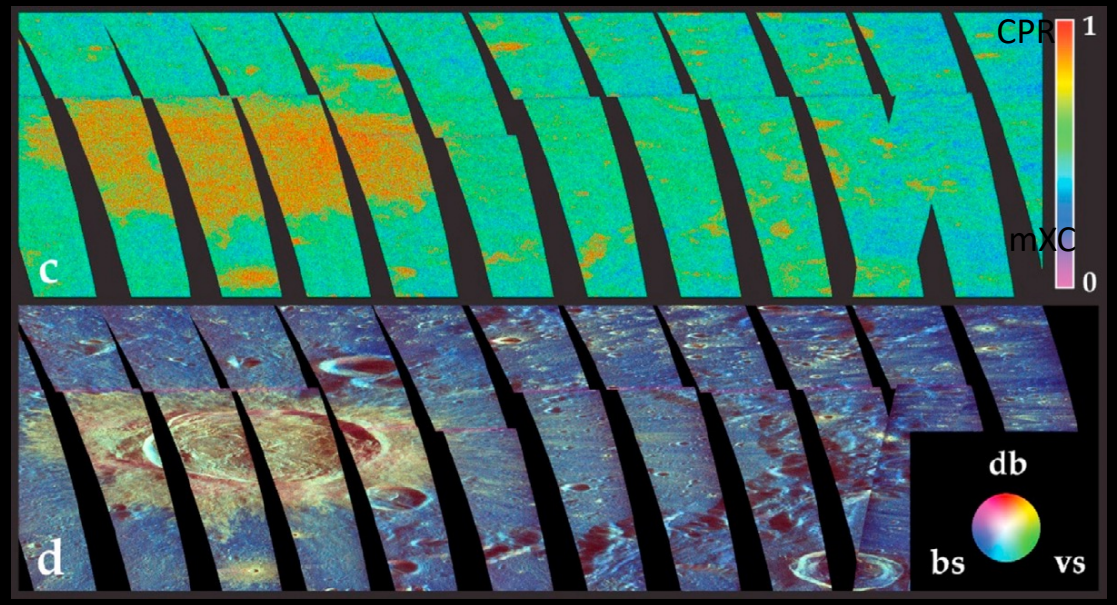

[Raney et al. 2012, JGR 17]

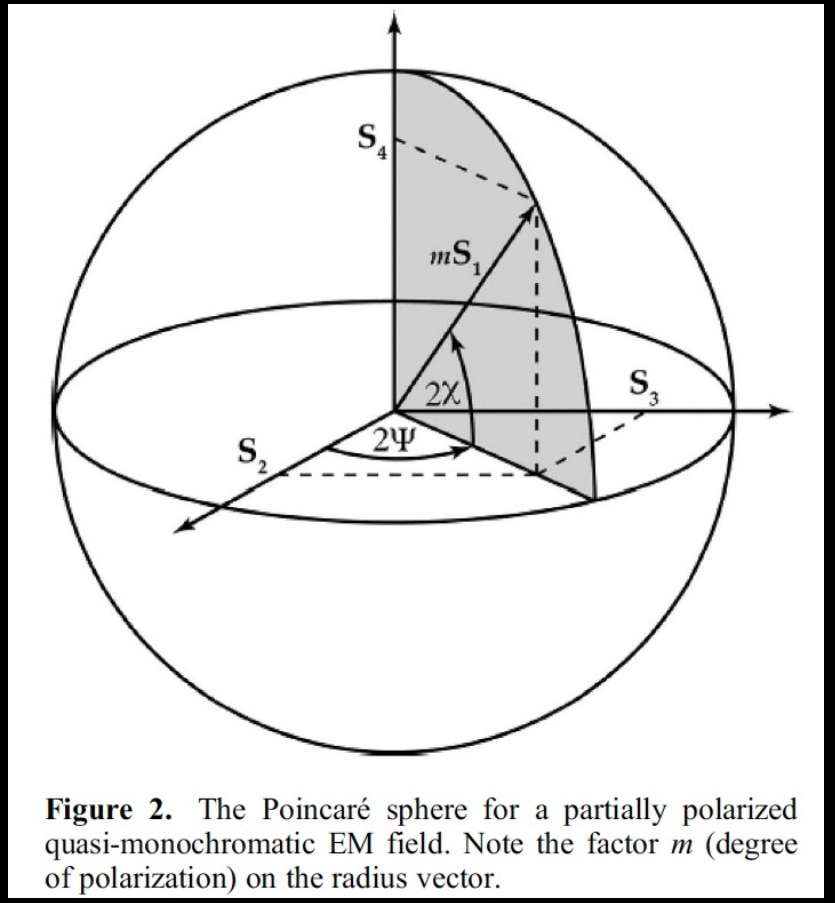

Figure 2. The Poincaré sphere for a partially polarized quasi-monochromatic EM field. Note the factor m (degree of polarization) on the radius vector.

Dihedral double bounce

Simple backscattering

Diffuse volume scattering

1999 JM8 (P type)

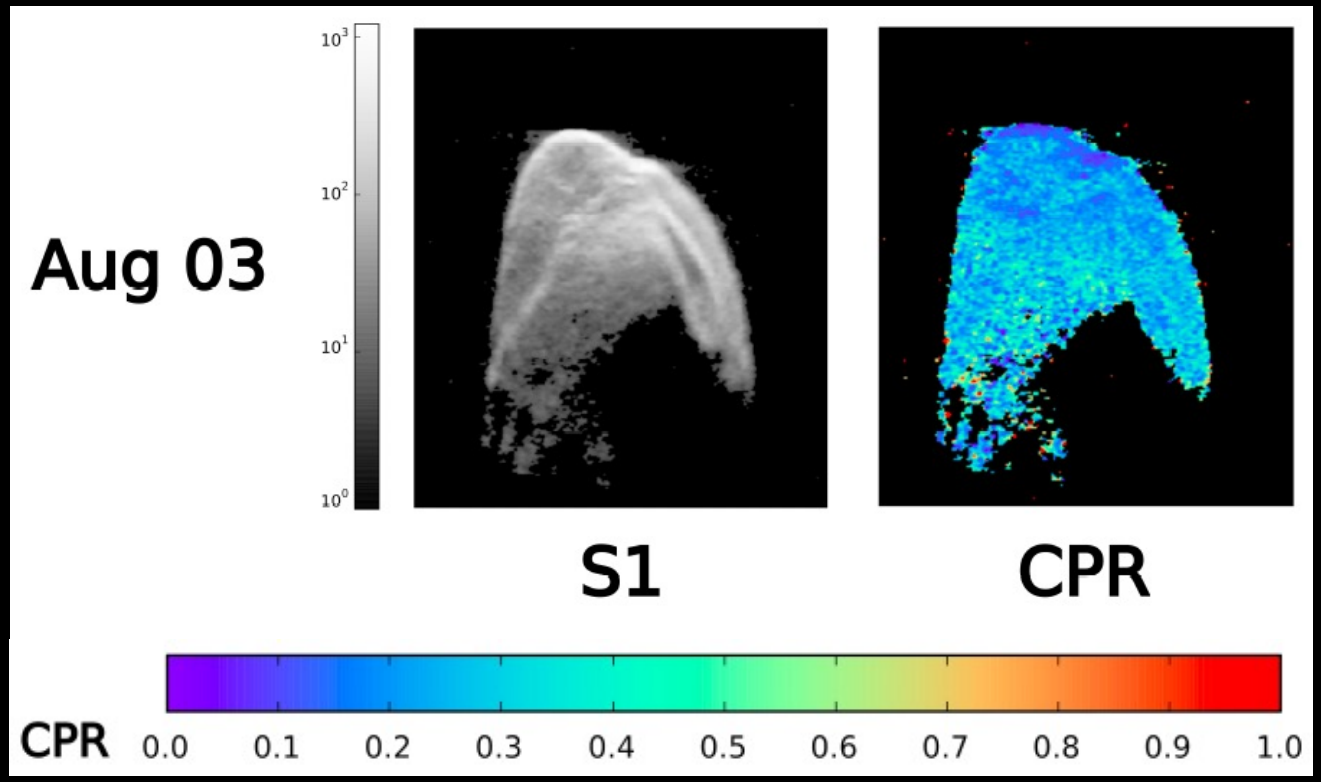

Low CPR all over, blue dominates
[Hickson et al. 2021]

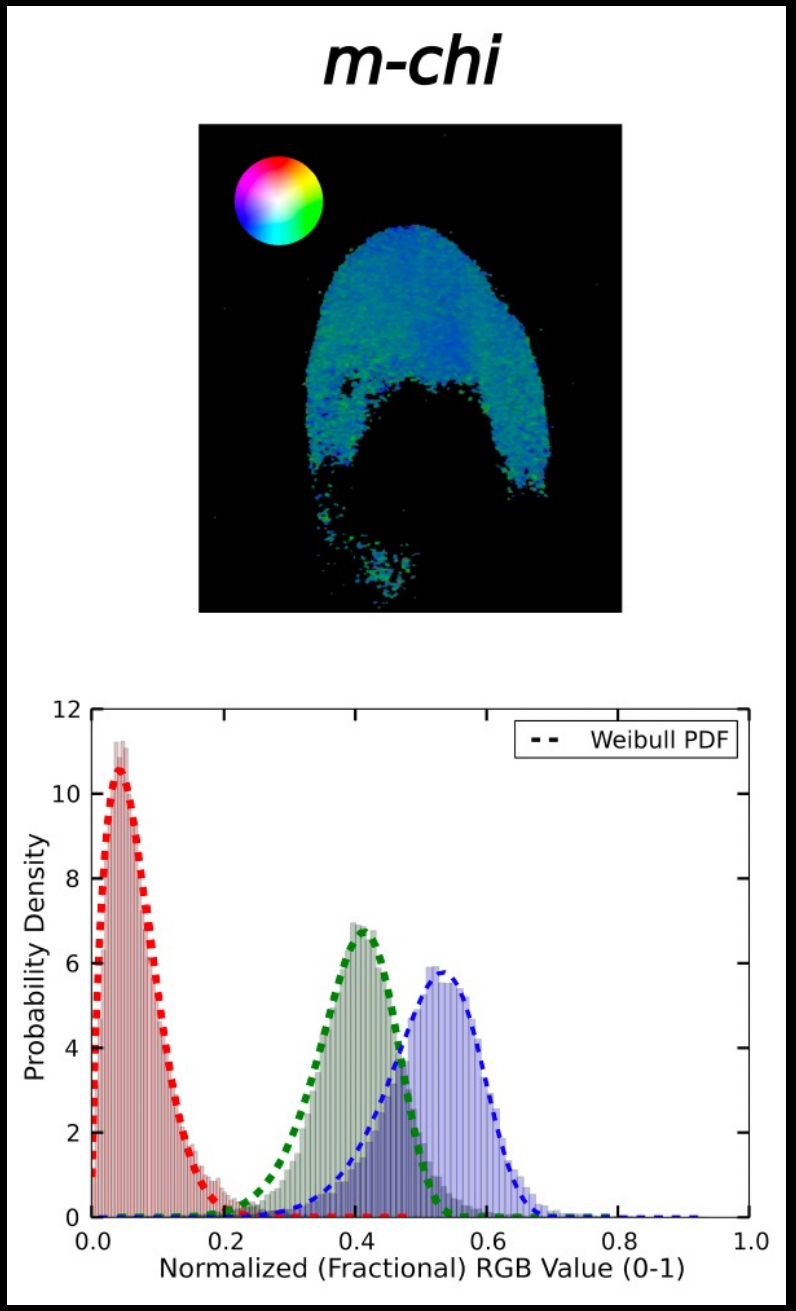

33342 1998 WT24 (E type)

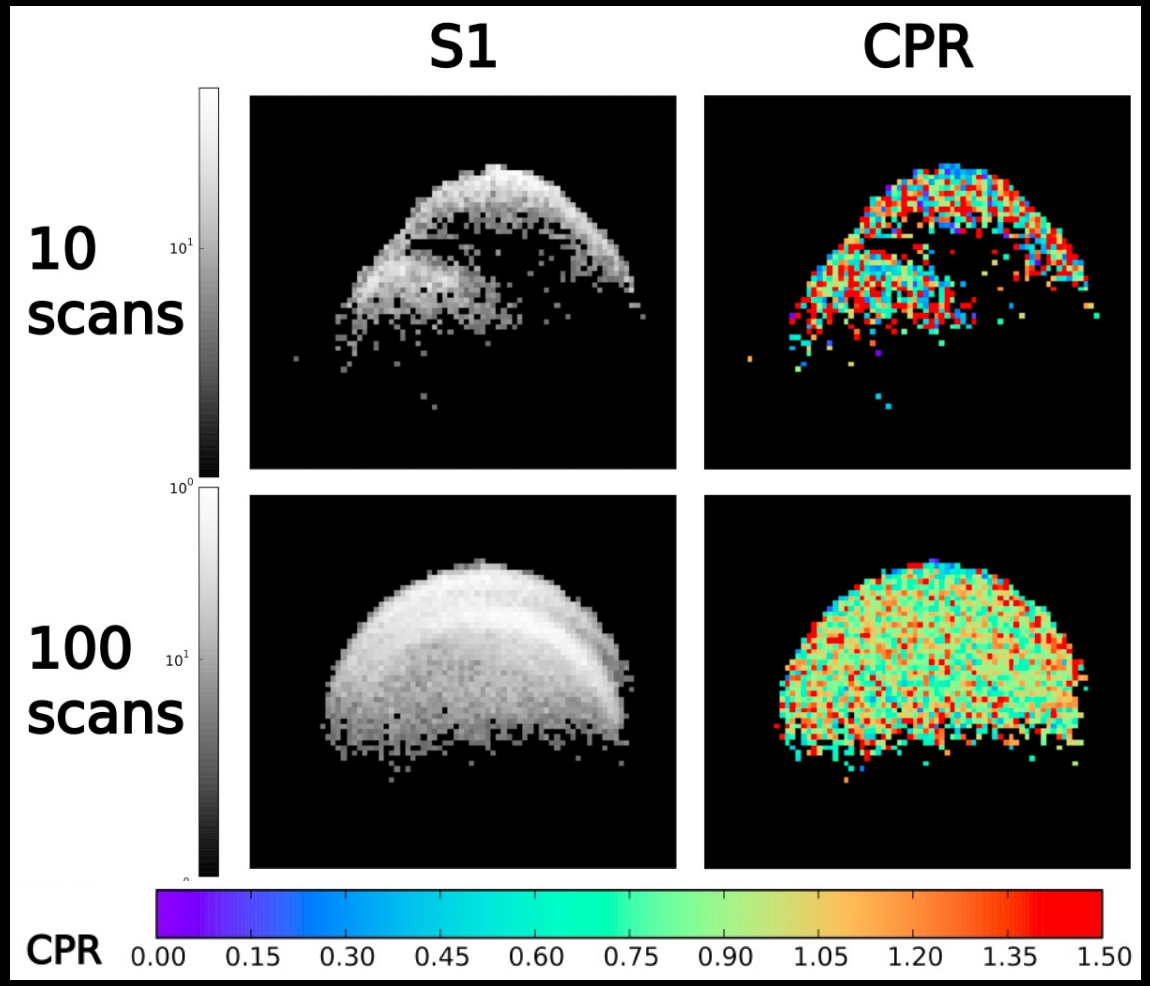

High CPR all over, green dominates, red nearly equal to blue [Hickson et al. 2021]

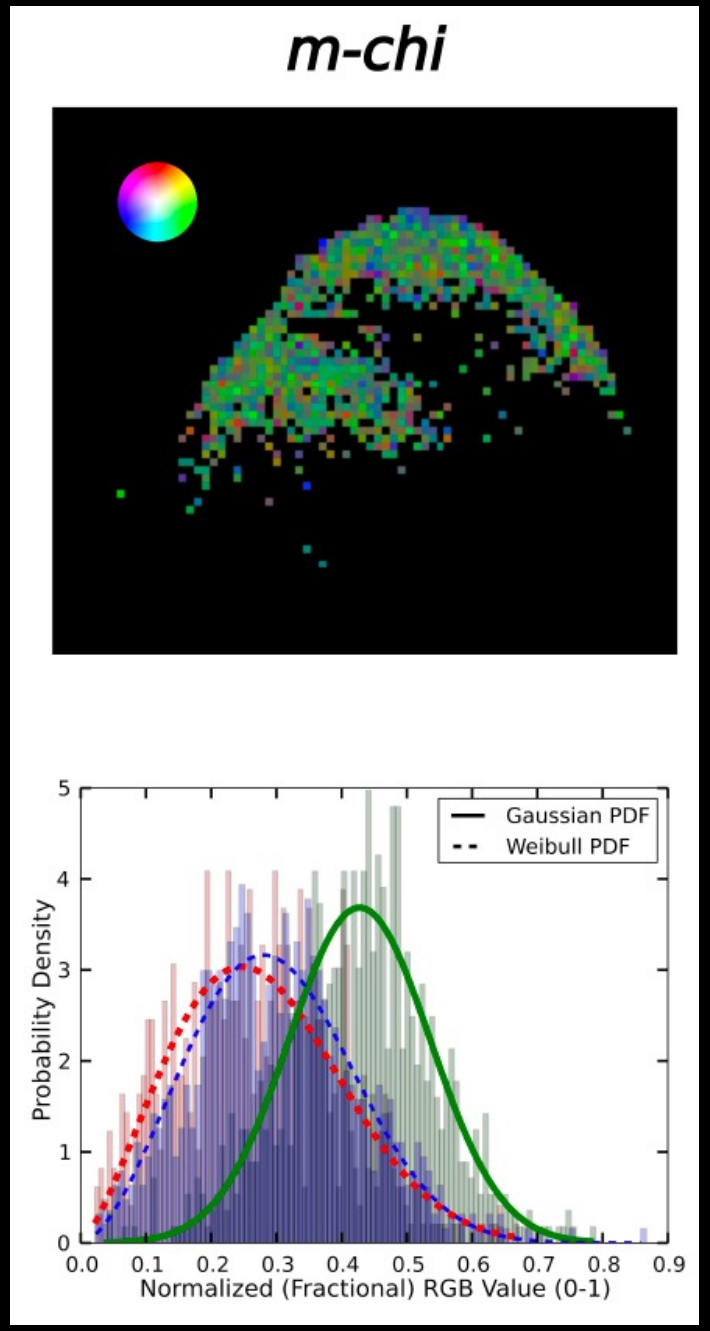

Penetration depth – Energy loss in a medium

An electric field's polarization component p can be written as

$$E_p(x) = a_p e^{-\alpha x} e^{-i\beta x}$$

where X is the travelled distance, the loss factor

$$\alpha = 2\pi f \sqrt{\varepsilon\mu[(1+t_\delta^2)^{\frac{1}{2}} - 1]/2},$$

and the phase factor

$$\beta = 2\pi f \sqrt{\varepsilon\mu[(1+t_\delta^2)^{\frac{1}{2}} + 1]/2}.$$

Here, f is the frequency of a wave in the medium where it is passing through, ε is the medium's effective complex electric permittivity (a.k.a. dielectric constant), μ is its magnetic permeability, and the loss tangent

$$t_\delta = \frac{\varepsilon''}{\varepsilon'} = \frac{\sigma}{2\pi f \varepsilon}$$

The primes indicate the real and imaginary parts of the dielectric constant so that

$$\varepsilon_r = \varepsilon' + i\varepsilon'' = (\varepsilon - i\frac{\sigma}{2\pi f})/\varepsilon_0$$

and σ is the conductivity. The permittivity of free space, $\varepsilon_0 = 8.85\times10^{-12}$ F/m.

Penetration depth – Energy loss in a medium

An electric field's polarization component p can be written as

$$E_p(x) = a_p e^{-\alpha x} e^{-i\beta x}$$

where x is the travelled distance, the loss factor

$$\alpha = 2\pi f \sqrt{\varepsilon\mu[(1+t_\delta^2)^{\frac{1}{2}} - 1]/2},$$

and the phase factor

$$\beta = 2\pi f \sqrt{\varepsilon\mu[(1+t_\delta^2)^{\frac{1}{2}} + 1]/2}.$$

For incident power given by P_0, the power remaining after distance x can be written as

$P_p(x) = \left|E_p\right|^2 = P_0 e^{-2\alpha x}$ (no phase term!)

The penetration depth is the distance where the power has been reduced to 1/*e, i.e.*

$$x = \frac{1}{2\alpha}$$

Attenuation is often described in units of dB/m. In regoliths, the penetration depth can be several wavelengths, less in metal-rich materials, or more in water ice.

Icy Galilean satellites

- Coherent backscattering effect can cause a significant enhancement to the backscatter efficiency in the right circumstances
- Multiple scattering in a low-absorption material (water ice in microwave frequencies with deposits of rocks, voids etc.)

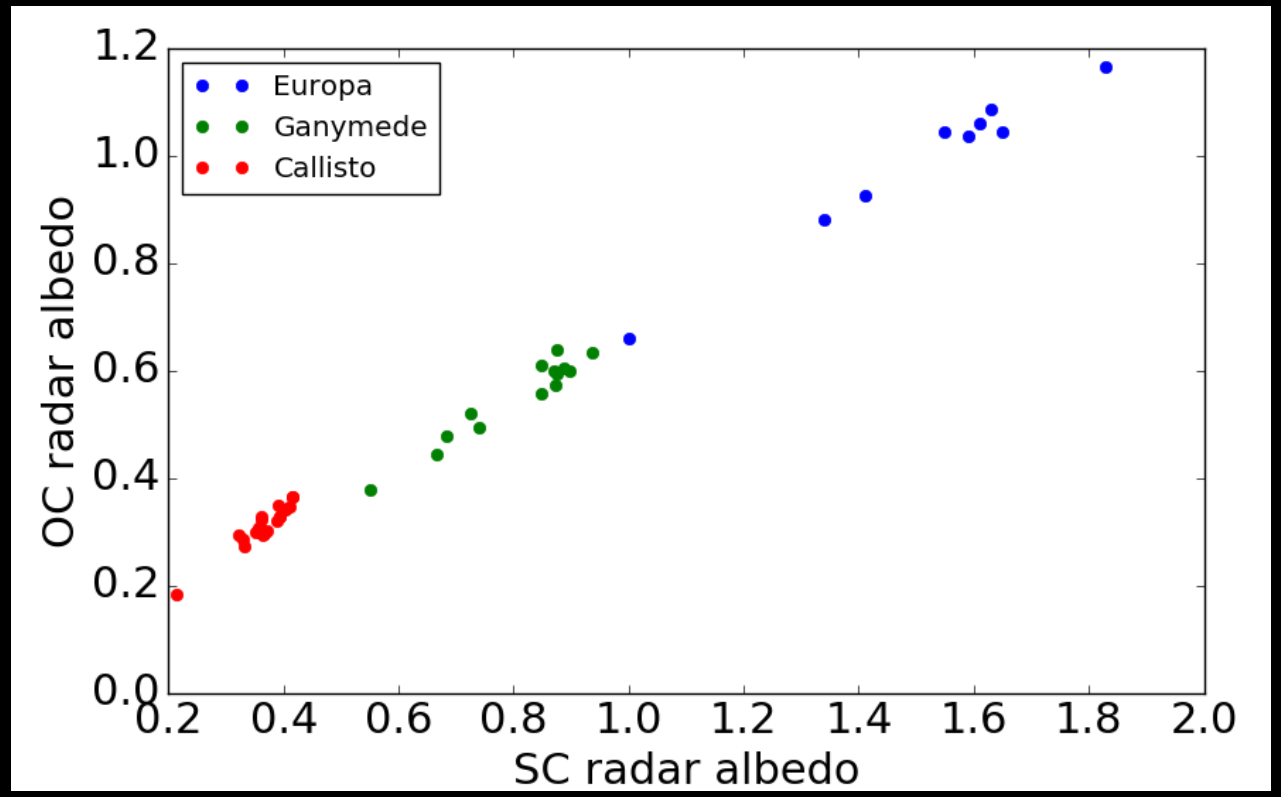

Mercury’s permanently shadowed craters

Mercury’s poles have permanently shadowed crater floors with thick layers of ice (confirmed by MESSENGER mission), which causes a very strong radar enhancement especially in the SC polarization.

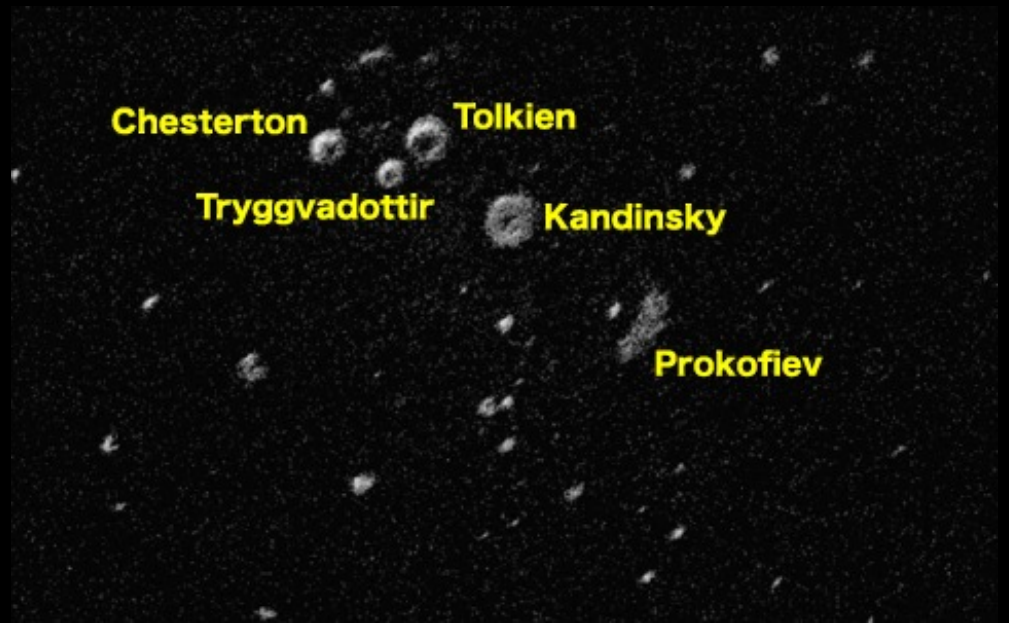

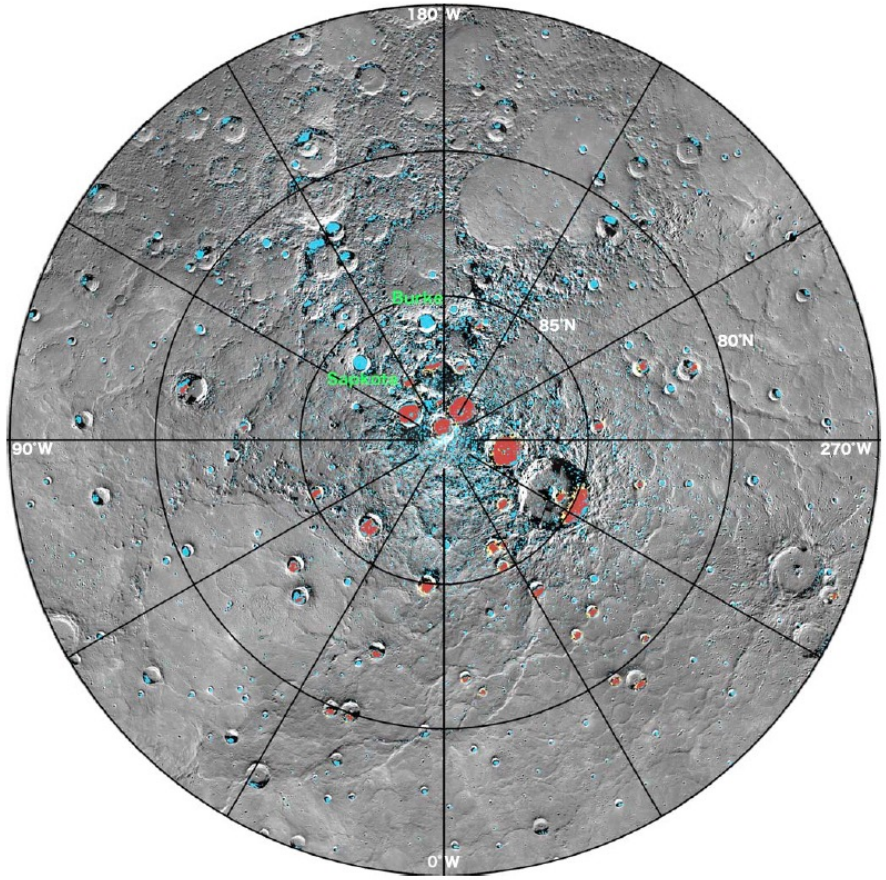

Figure 3. Overlay of the DBSCAN-identified radar-bright features (yellow) onto a MESSENGER MDIS map of the northern polar terrain. In cyan, we show the MESSENGER-constrained locations of areas within craters that are in permanent shadow. Areas where radar-bright features coincide with a PSR appear in brick orange. The Sapkota and Burke craters are labeled in green. The map is limited to latitudes >75°N. Over the six-day observing run, the radar beam is on average illuminating the area from the direction of 321°W.

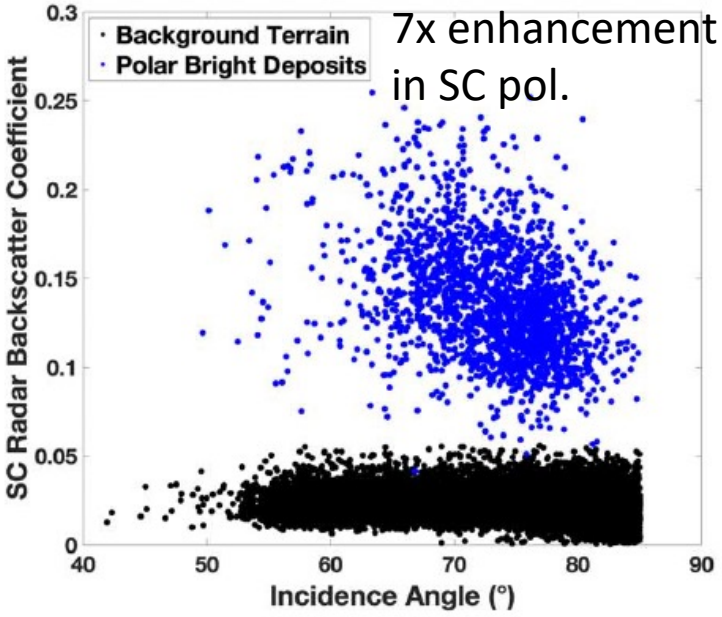

7x enhancement in SC pol.

(a)

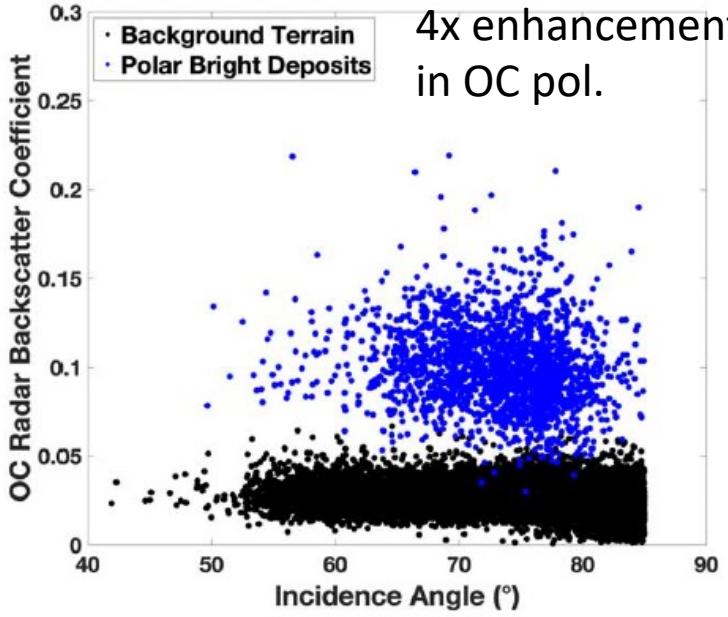

4x enhancement in OC pol.

(b)

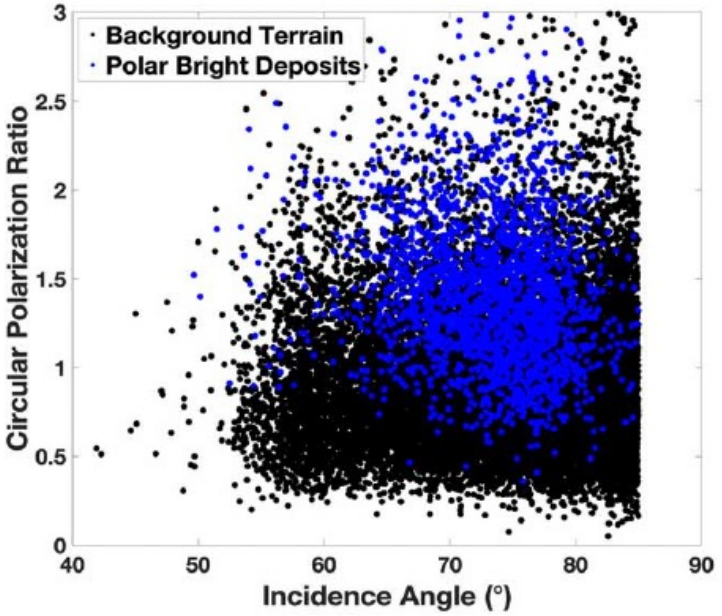

(c)

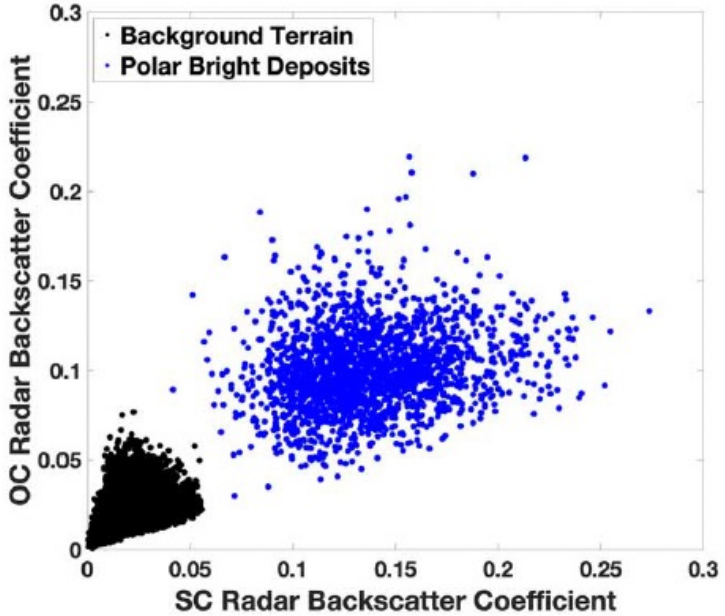

(d)

Rubble vs. bulk surface in the disk functions

- The observed BSC is a combination of the reflections from the undulating surface and the wavelength-scale particles (“boulders”) in the subsurface and on the surface
- On the right, a model including both of these compared to the radar disk function of the Moon

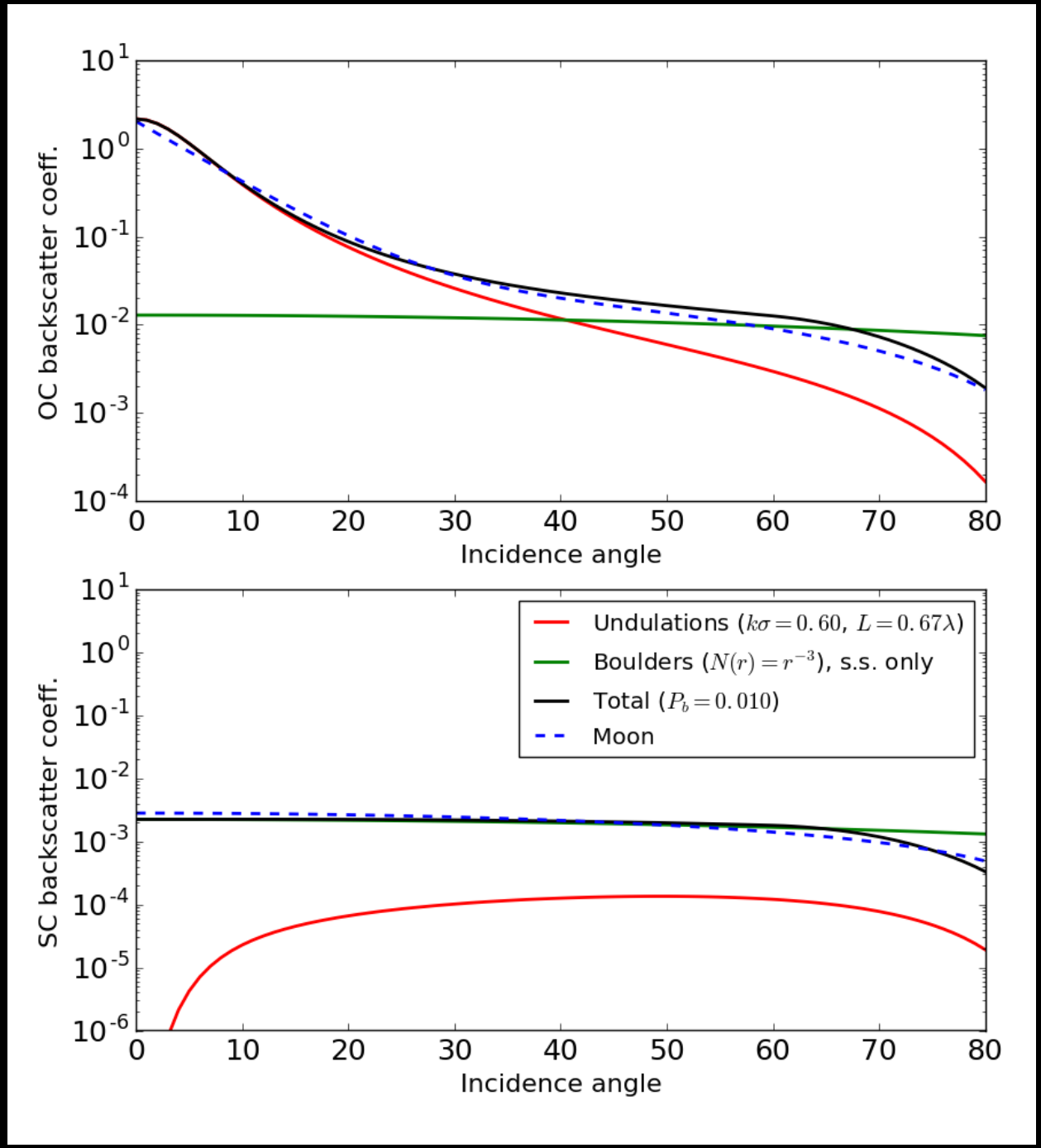

Scattering by irregularly-shaped wavelength-scale particles

On the left: Scattering matrix elements 1-1, 1-2, 2-2, and 4-4 as a function of scattering angle using different materials and particle shapes (spheres vs. irregular shapes)

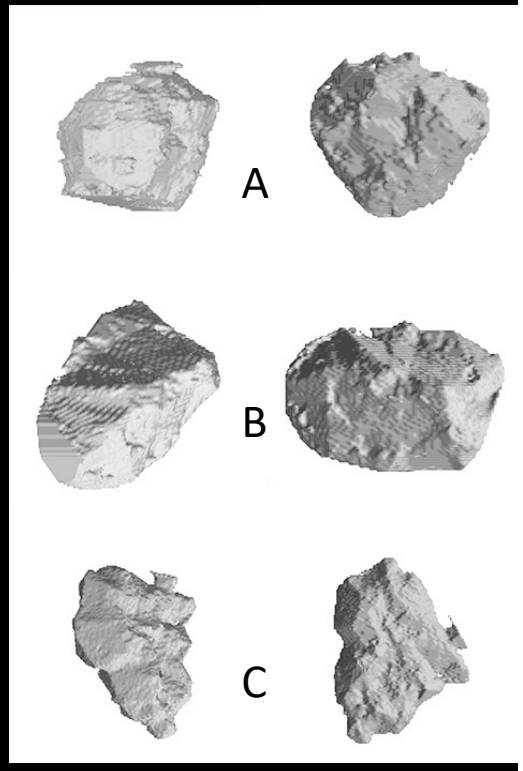

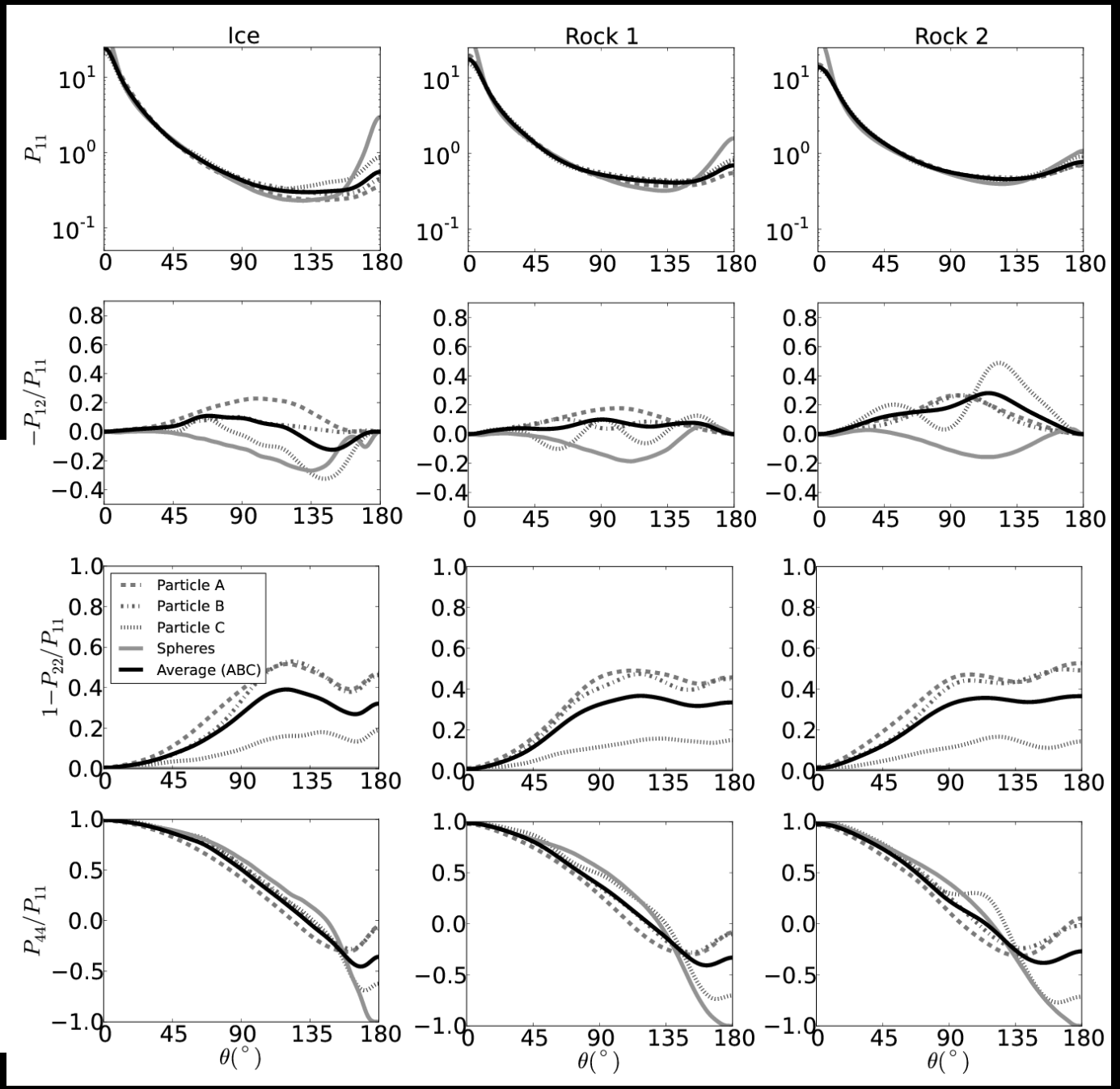

m-chi decomposition of wavelength-scale particles (rubble)

Size parameter $= \frac{\pi D}{\lambda}$

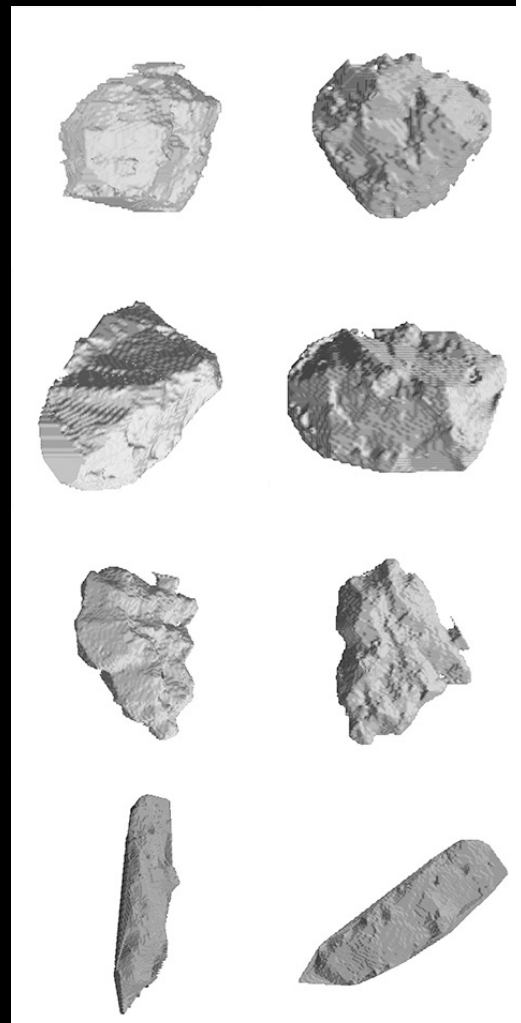

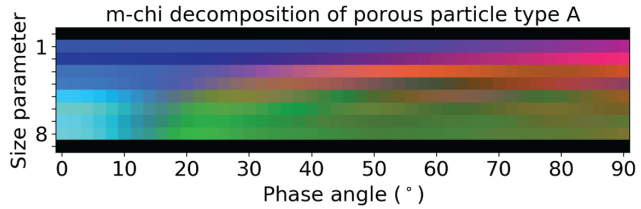

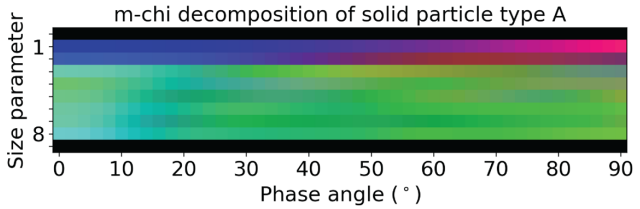

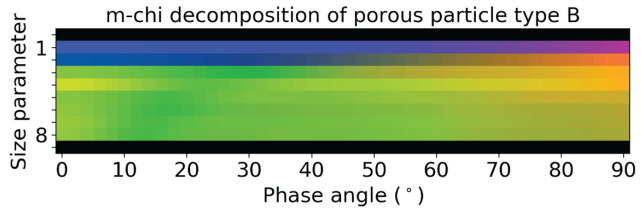

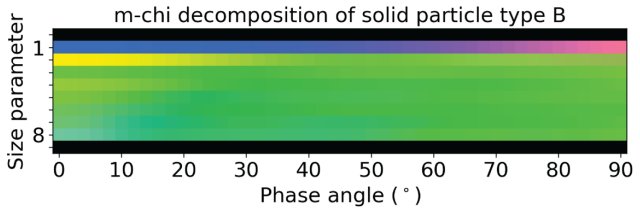

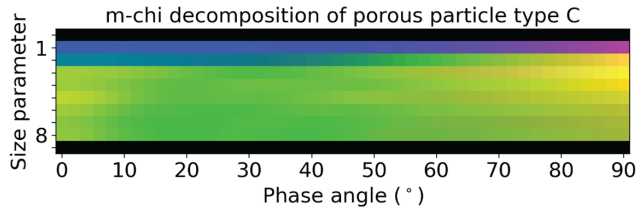

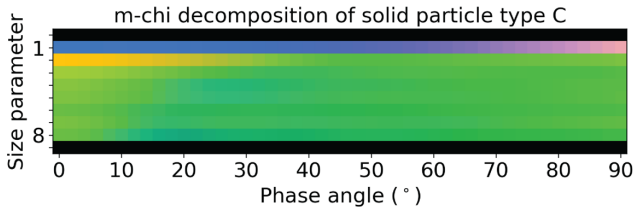

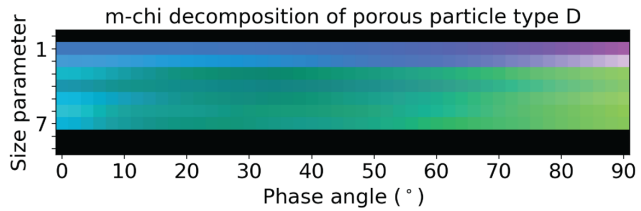

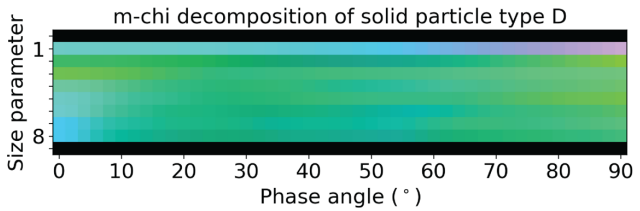

Effect of the rubble on the radar albedo and polarization properties

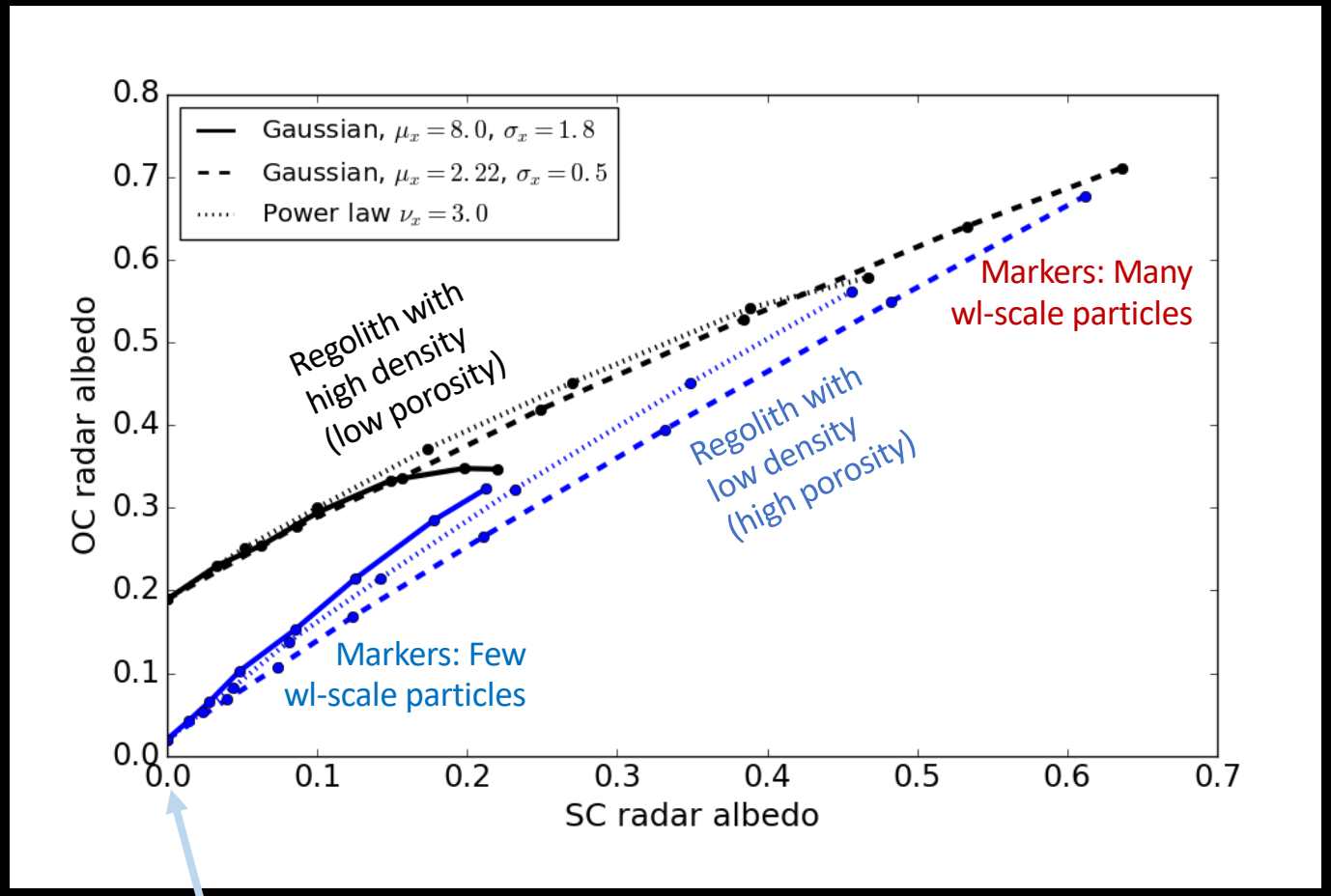

The axis intersection point is related to the electric permittivity through the Fresnel reflection coefficients

$\hat{\sigma}_C > \hat{\sigma}_s$ at high incidence angles

Effective radar BSC of wl-scale particles (requires computing)

Effective radar BSC of fine-grained regolith*

$$\hat{\sigma}(\theta) \sim P_C(\theta)\hat{\sigma}_C + [1 - P_C(\theta)]\hat{\sigma}_m(\theta)$$

Probability of the observed scattering contribution by a wl-scale particle

*Sub-wl-scale particles (radius $r \ll \lambda$):

$$\hat{\sigma} = 4k_m^4 r^4 \left|\frac{\varepsilon - 1}{\varepsilon + 2}\right|^2$$

Radar albedo vs. SC/OC ratio

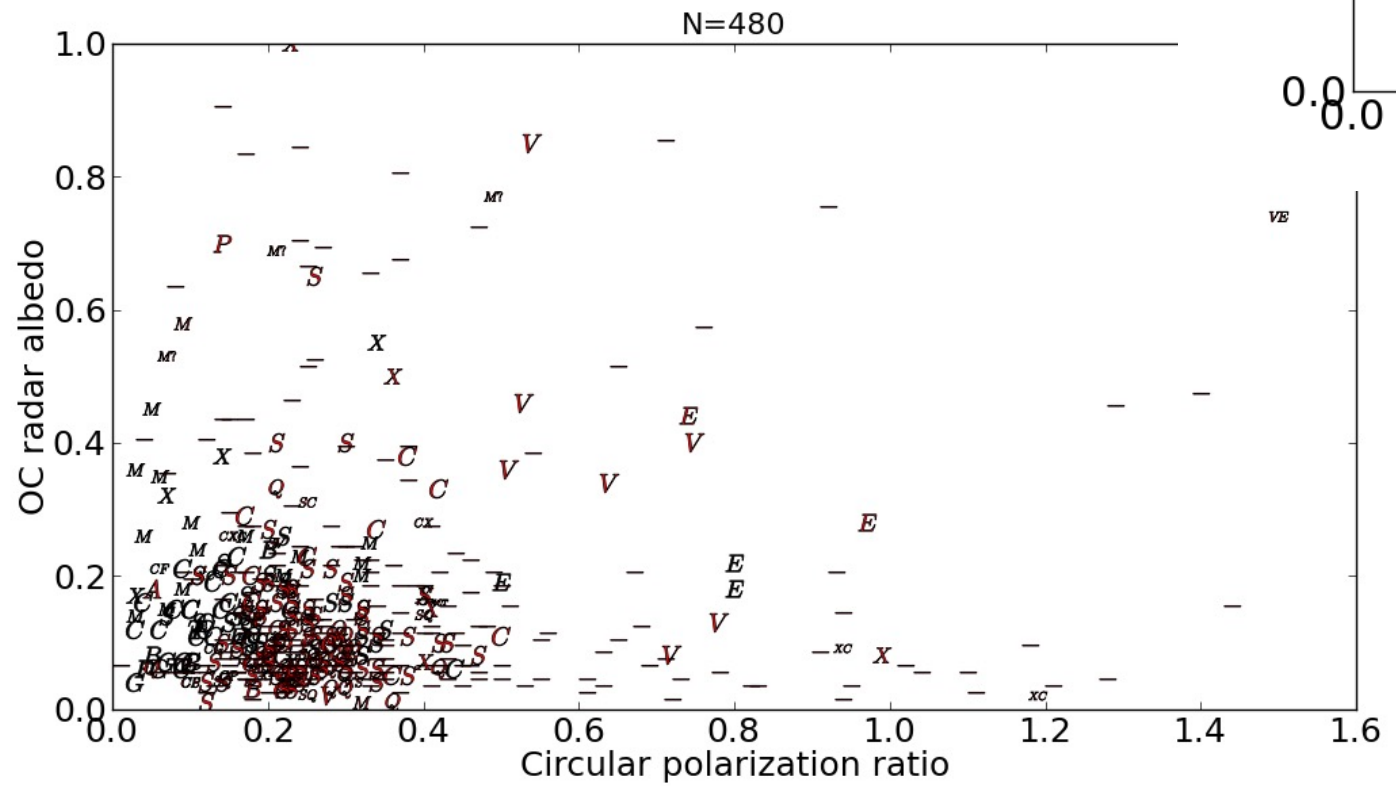

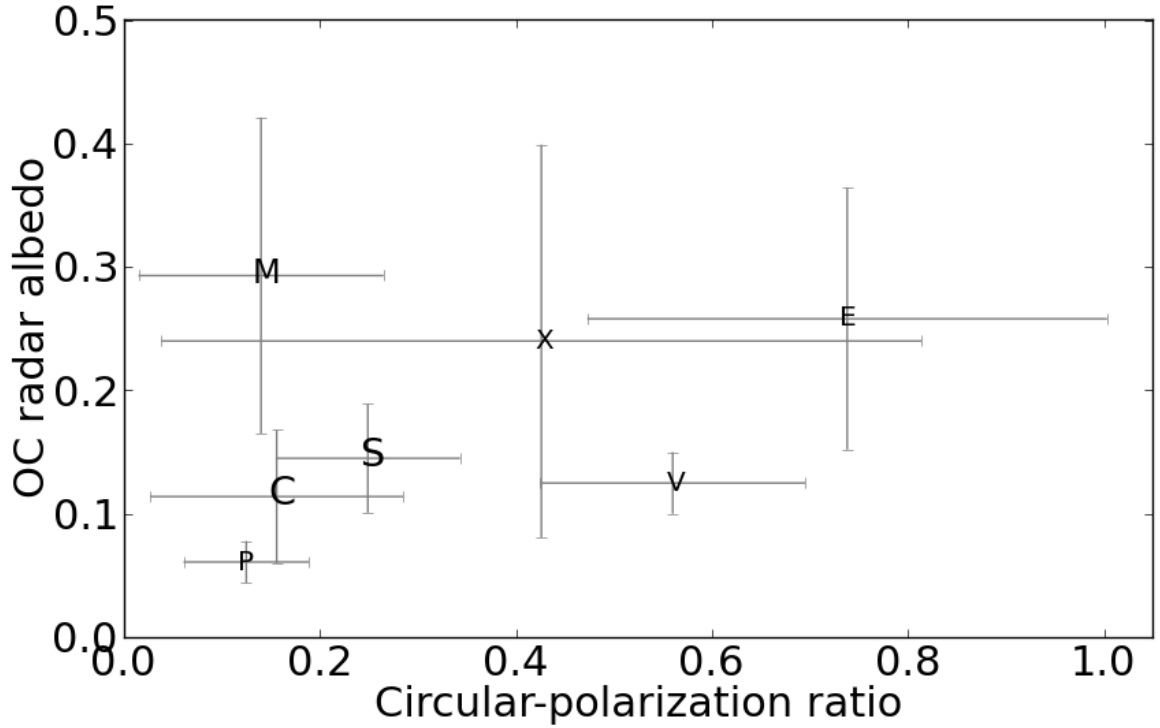

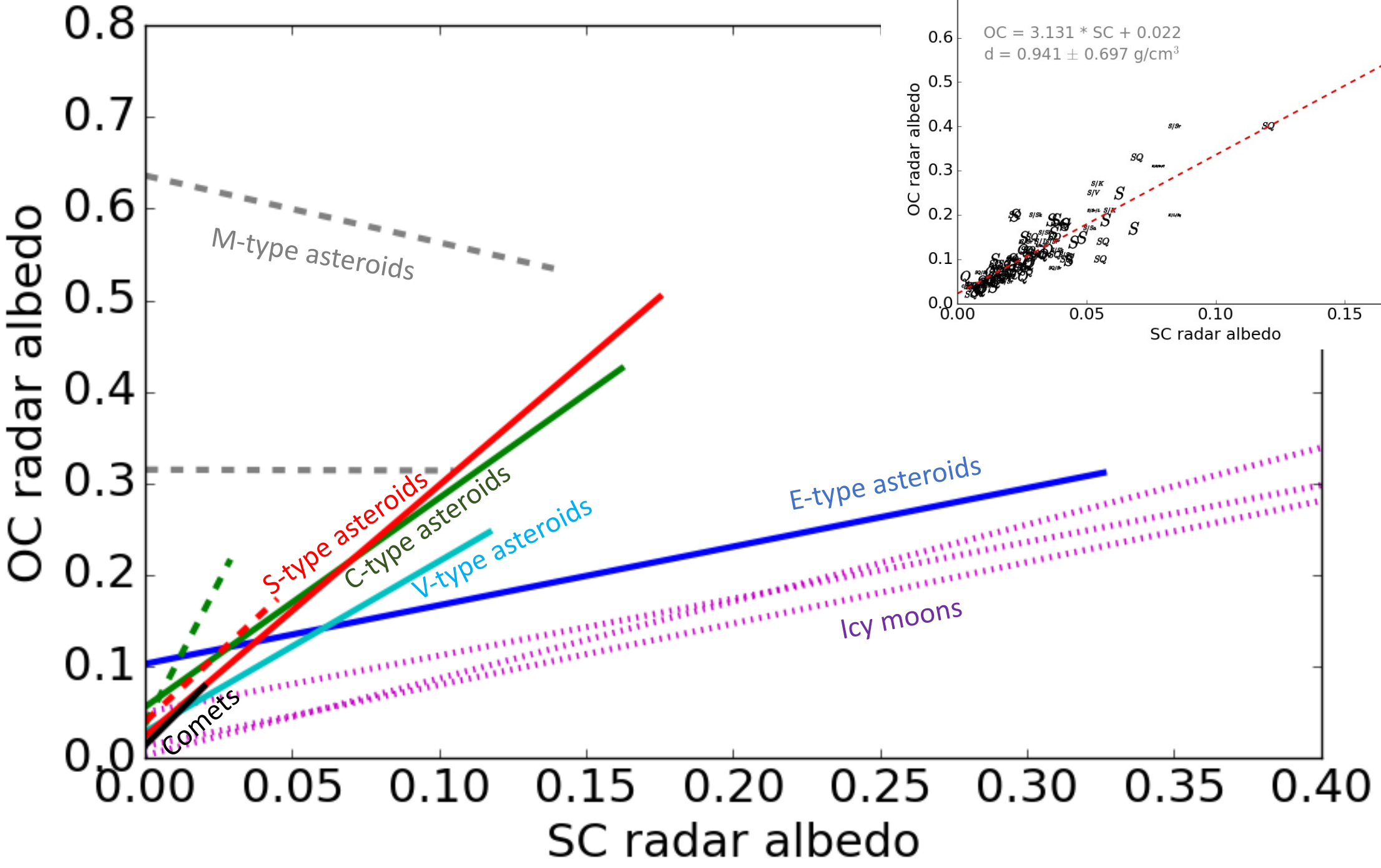
OC radar albedo
SC radar albedo
M-type asteroids
S-type asteroids
C-type asteroids
V-type asteroids
E-type asteroids
Icy moons
Comets
OC = 3.131 * SC + 0.022
d = 0.941 ± 0.697 g/cm³
OC radar albedo
SC radar albedo

Effect of the rubble on the radar albedo and polarization properties – particle shapes

The markers show the fraction of the surface covered by the particles: Each one is +10 %.

Dirty ice or porous particles

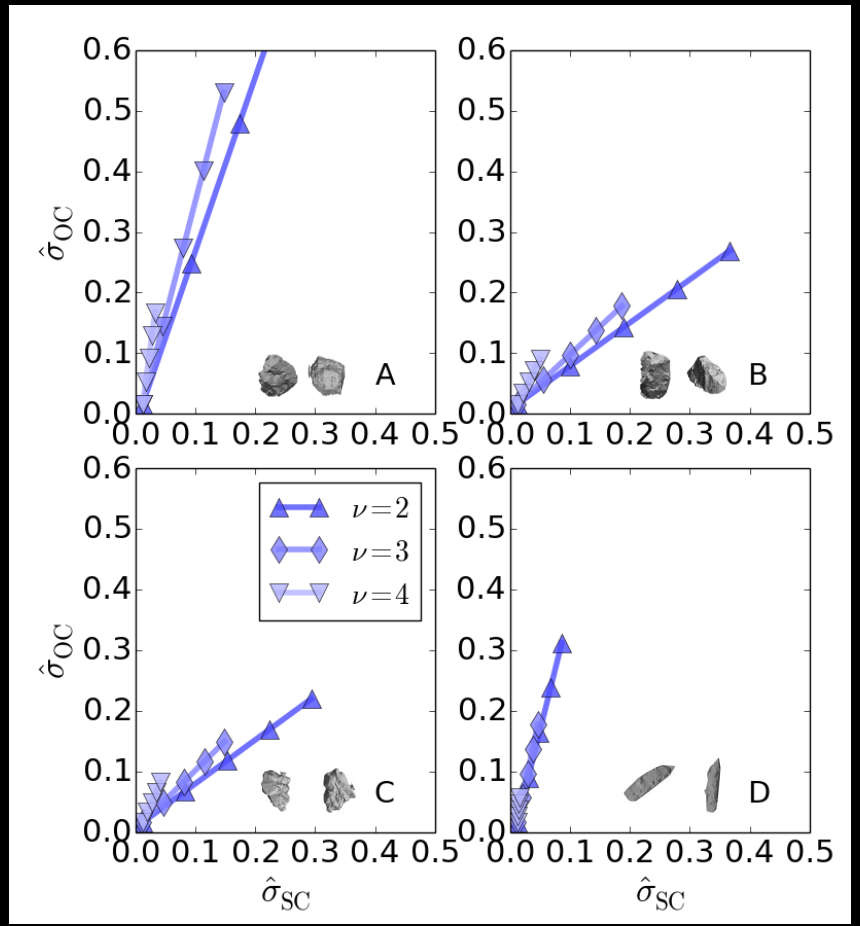

Solid silicates

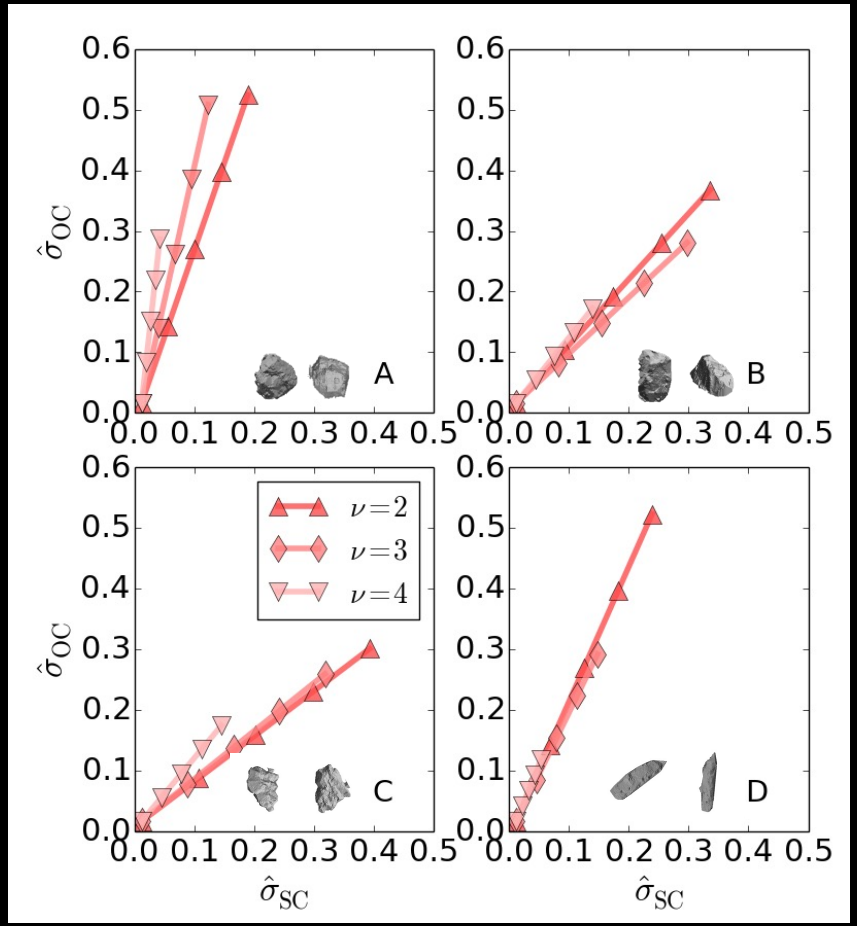

The Moon through Mini-RF

- Analysis of 27 craters from around the Moon
- External vs. internal regions
- Reflectivity in the same and opposite sense polarizations (SC & OC) vs. the circular-polarization ratio (SC/OC)
- Observed using a spacecraft radar system, incidence angle ~50° (directions shown by arrows in the panel corners)

[Virkki & Bhiravarasu, *JGR Planets 2019*]

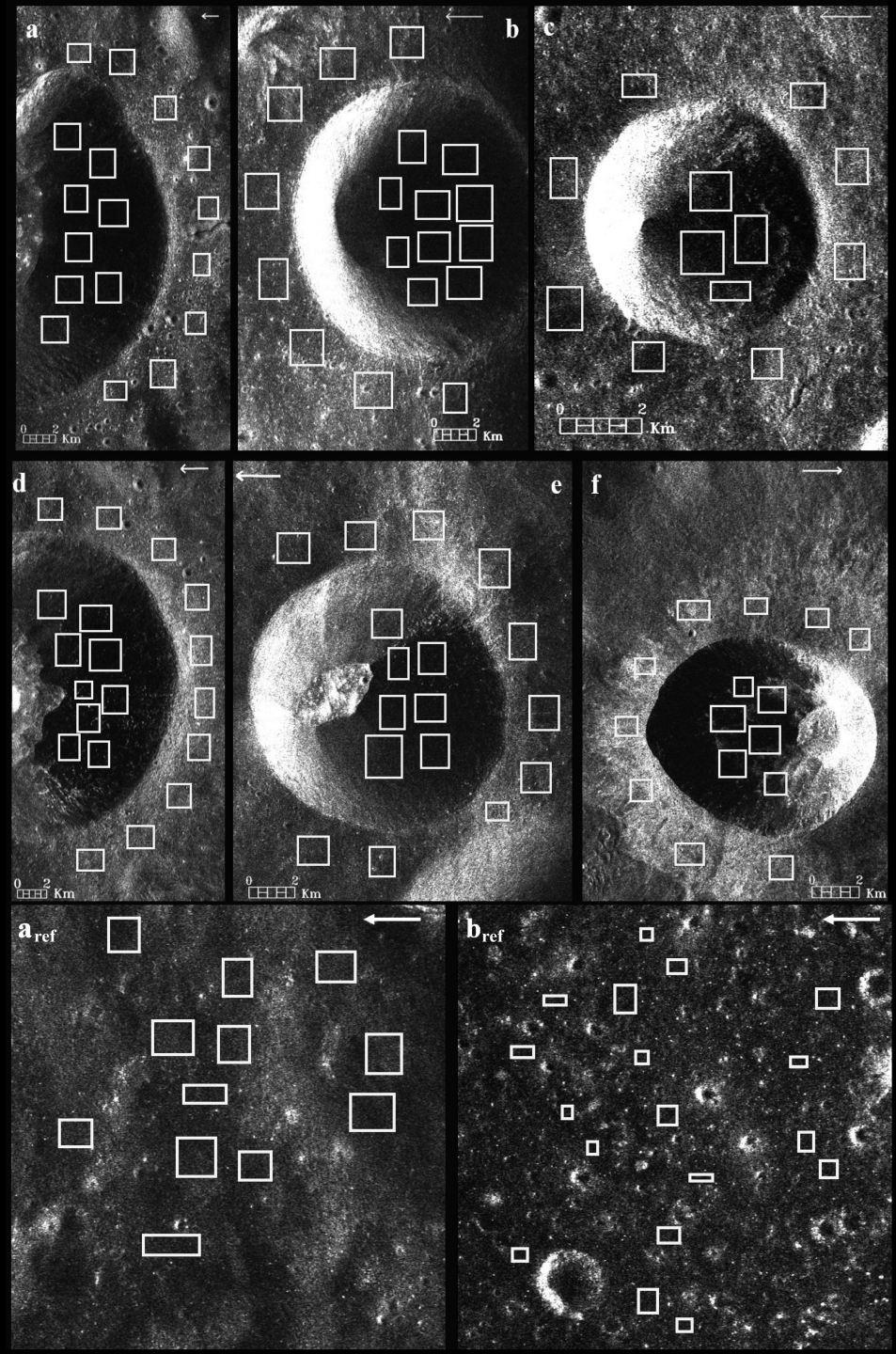

The Moon through Mini-RF

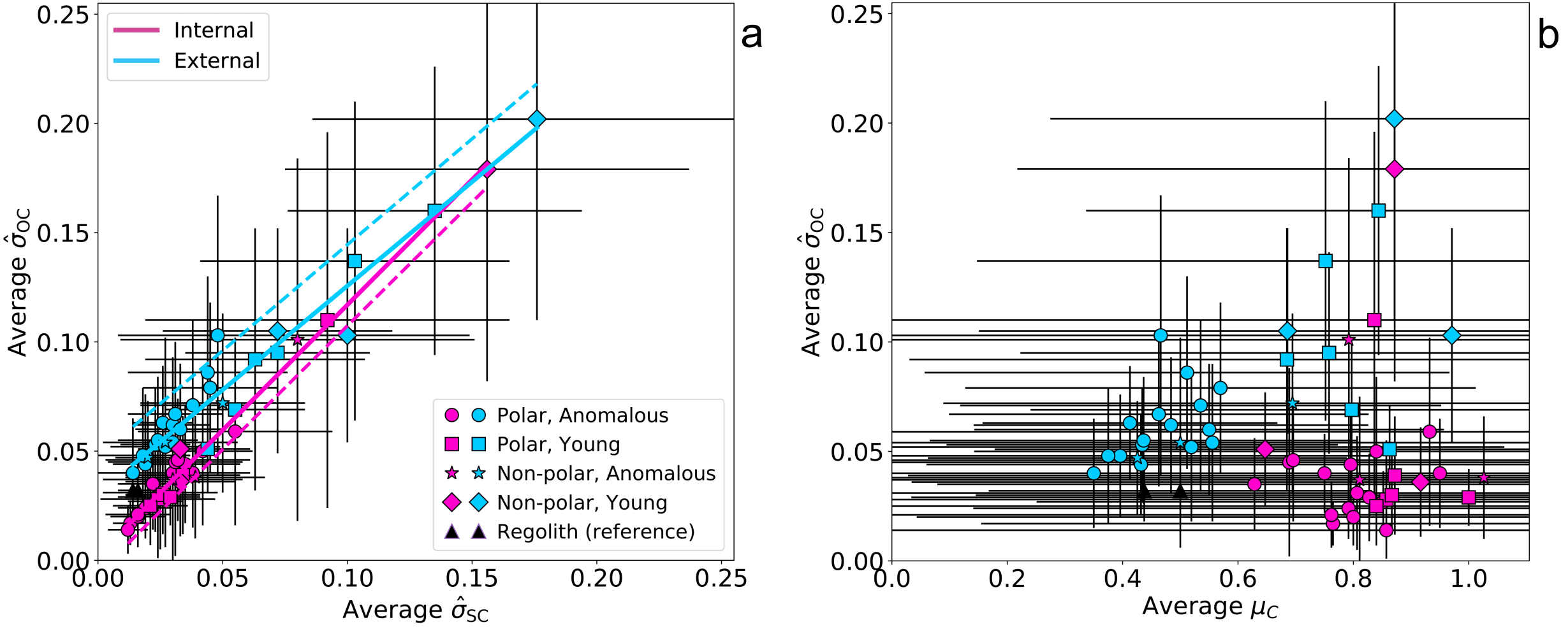

Venus in radar

A. Magellan HH polarization
B. Earth-based OC polarization
C. Earth-based SC polarization

- The white outline in (A) denotes the parabolic deposit extent measured by Campbell et al. (1992). Note that the radar-dark deposits of the 31-km crater Aurelia can be traced across the melt flows of the 63-km crater Seymour in the HH and OC images, but the greater attenuation of the SC echoes in the rough melt flow terrain reveals a more contiguous regional mantling.
- Radar-dark regions can have two interpretations: Less wavelength-scale particles than the surrounding regions (if SC is darker as well) or a lower effective permittivity (if SC is not anomalously low)

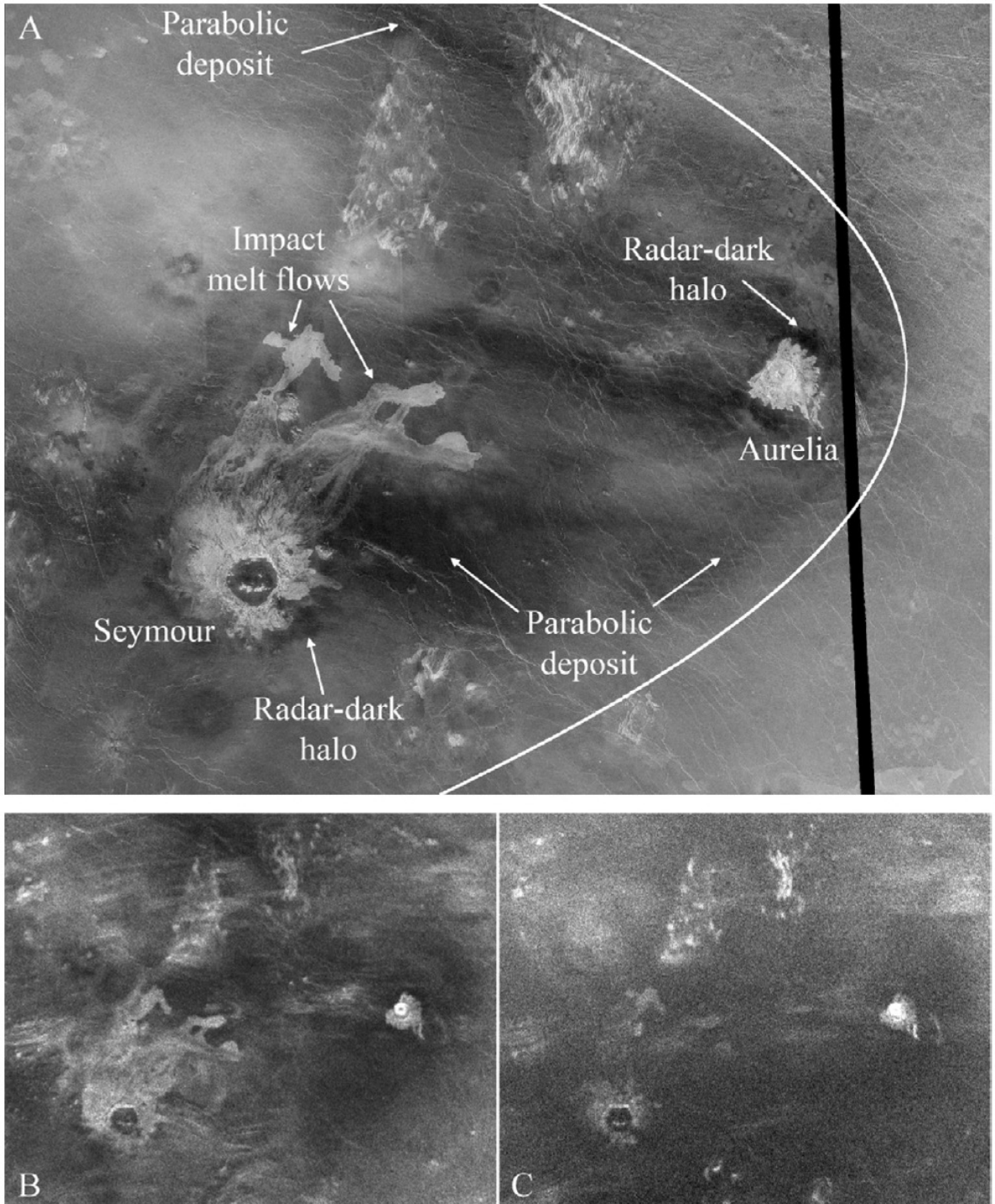

Vector Radiative Transfer model

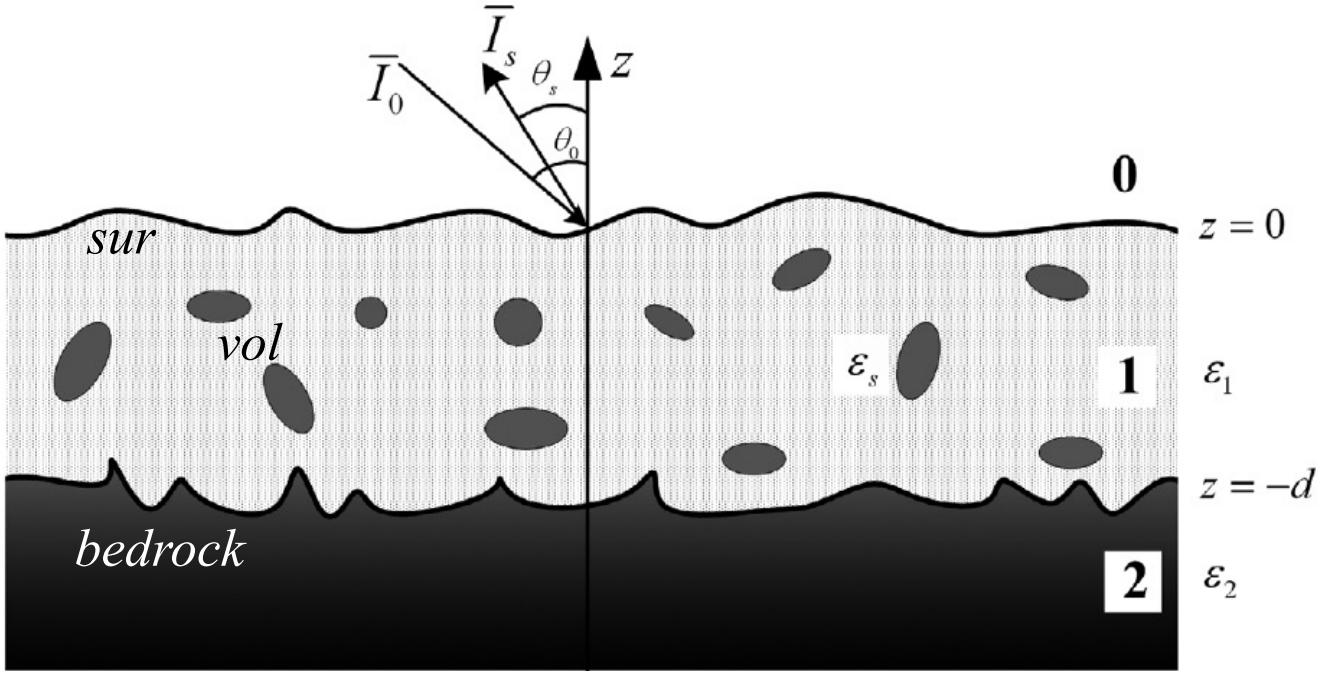

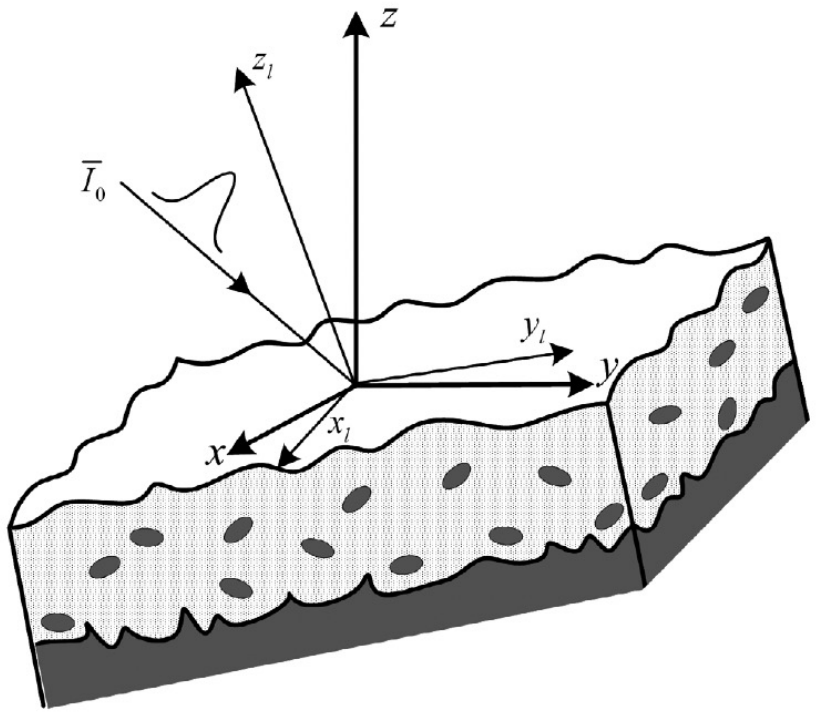

$$\bar{I}_s(\theta,\phi,z=0) = \bar{I}_{sur}(\theta,\phi,z=0) + \bar{I}_{bedrock}(\theta,\phi,z=0) + \bar{I}_{vol}(\theta,\phi,z=0) + \bar{I}_{bedrock\_vol}(\theta,\phi,z=0) + \bar{I}_{vol\_bedrock}(\theta,\phi,z=0)$$

[Fa et al. 2011]

Vector Radiative Transfer model

Parameters	Definition	Typical Value	Reference
d	regolith thickness	4–5 m for the maria, 10–15 m for the highlands	*McKay et al.* [1991]
δ_1, l_1	root mean square height and correlation length of surface	not available	
δ_2, l_2	root mean square height and correlation length of subsurface	not available	
$s_1 = \sqrt{2}\delta_1/l_1$	1-D root mean square slope of surface	2°–4° for the maira, 6°–8° for the highlands	*Tyler and Howard* [1973]
$s_2 = \sqrt{2}\delta_2/l_2$	1-D root mean square slope of subsurface	not available	
f_s	fractional volume of buried inclusions	0–0.1 based on rocks at the Surveyor landing sites	*Thompson et al.* [1970]
c, a	semimajor and semiminor axes of the buried inclusions	several mm to tens of cm	*Thompson et al.* [1970]
ε_1, ε_2, ε_s	dielectric constant of regolith, underlying bedrock, and rocks	bulk density and composition dependent	*Carrier et al.* [1991]
ε_{ice}	dielectric constant of ice	3.15 + i(0.0001–0.1)	*Cumming* [1952], *Evans* [1965], and *Ray* [1972]
ρ	regolith bulk density	1.3–2.0 g/cm^3	*Carrier et al.* [1991]
S	FeO+TiO_2 abundance of regolith	0–30 (wt. %)	*Lucey et al.* [2000], *Lawrence et al.* [2002], and *Prettyman et al.* [2006]

Vector Radiative Transfer model – An example of results

- The OC and SC polarization components of BSC and their ratio as functions of different parameters (here regolith thickness and electric permittivity, while the permittivity of the submerged particles remains at 6 + 0.01i?
  - Regolith thickness varies up to 20 m
  - Regolith electric permittivity varies from 2 to 6
- Contributions of the surface, subsurface, volume, and subsurface-to-volume components to the total backscatter coefficient can be separated

Vector Radiative Transfer model

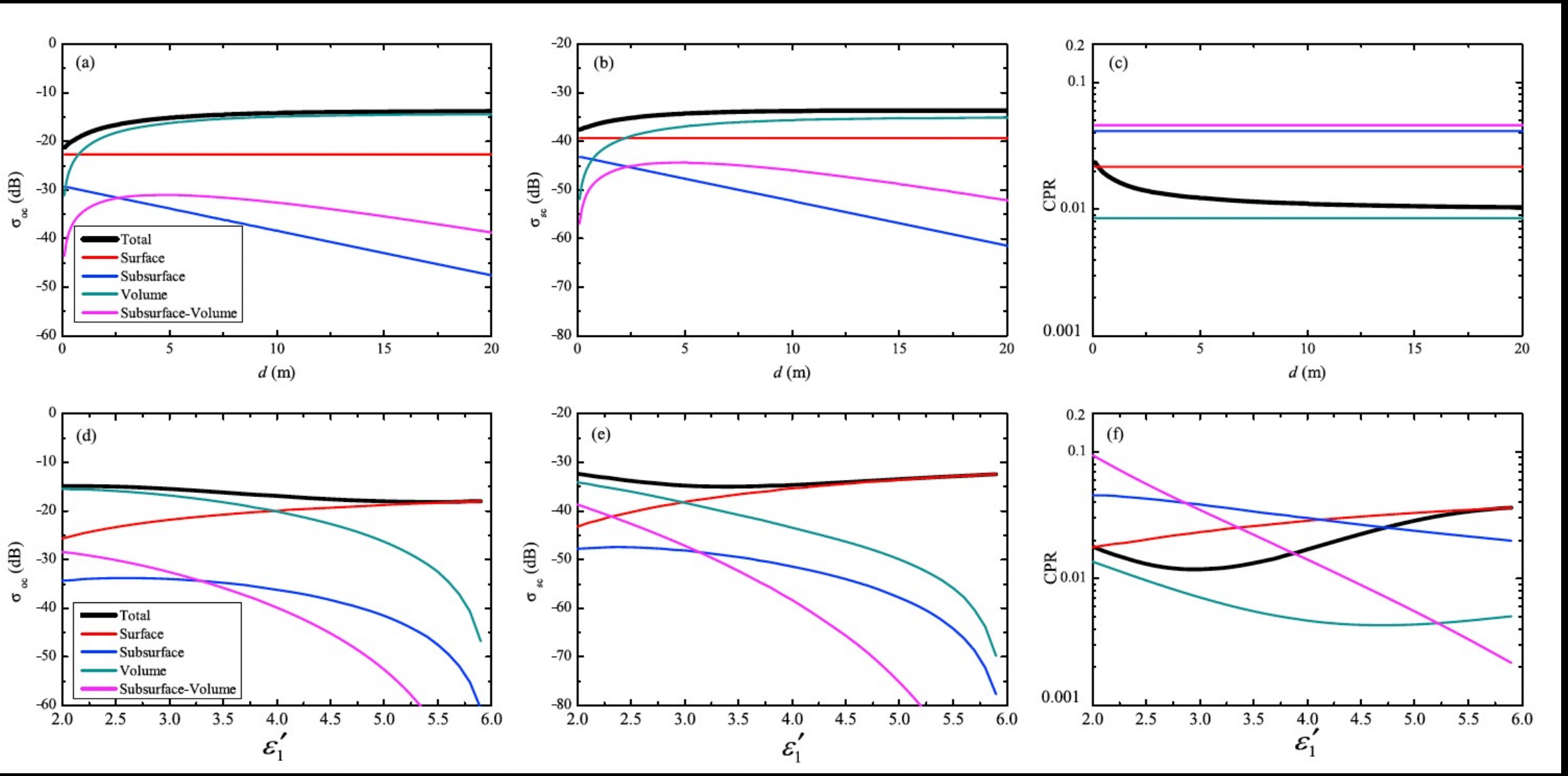

Summary

- Radar signals that encounter an interface between two media are split into reflected and transmitted components, whose amplitudes and polarization depend upon the dielectric properties of the media
  - The geometry of the surface is part of the electric property distribution
- Backscatter coefficient (BSC) describes the reflectivity of an area element, disk function describes BSC as a function of a incidence angle
- Radar echos are typically described by a two-letter code designating the transmitted and received polarization (linear: H/V; circular: L/R or SC/OC)
- The time- and ensemble averaged properties of the scattering medium can be represented using scattering matrices
  - M-chi decomposition is one way of illustrating the intensity and polarization distribution
  - Representing different scattering mechanisms with different matrices is sometimes helpful
- Natural materials have a non-zero conductivity that causes attenuation
  - Metal-rich materials have a high conductivity, water ice has a very low conductivity